AD 749972

SEISMIC DETERMINATION OF GEOLOGICAL DISCONTINUITIES AHEAD OF RAPID EXCAVATION

FINAL TECHNICAL RERORT

September 1972

D D C

RECEIVED

OCT 18 1972

B

DOCUMENT CONTROL DATA · R&D

(Security classification of title, body of abstract and indexing annotation must be entered when the overall report is classified)

1. ORIGINATING ACTIVITY (Corporate author)	2a. REPORT SECURITY CLASSIFICATION
Bendix Research Laboratories Bendix Center Southfield, Michigan 48076	Unclassified
	2b. GROUP

3. REPORT TITLE

Seismic Determination of Geological Discontinuities
Ahead of Rapid Excavation

4. DESCRIPTIVE NOTES (Type of report and inclusive dates)
Final Technical Report – 30 April 1971-31 July 1972

5. AUTHOR(S) (Last name, first name, initial)

Gupta, R. R.

6. REPORT DATE	7a. TOTAL NO. OF PAGES	7b. NO. OF REFS
August 1972	82	14

8a. CONTRACT OR GRANT NO. H0210033	9a. ORIGINATOR'S REPORT NUMBER(S)
b. PROJECT NO. ARPA Order No. 1579, Amend. 2	6311
c. Program Code 1F10	9b. OTHER REPORT NO(S) (Any other numbers that may be assigned this report)
d.	

10. AVAILABILITY/LIMITATION NOTICES

11. SUPPLEMENTARY NOTES BRL Project 2412	12. SPONSORING MILITARY ACTIVITY Advanced Research Projects Agency Washington, D.C. 80225

13. ABSTRACT

The need for the on-site knowledge of large geological discontinuities ahead of rapid excavation is very desirable so that hazardous or difficult formations ahead of an excavation face can be avoided or prepared for. Such information could result in fewer machine breakdowns, proper preparation for entry into zones where special precautions must be taken, and considerable savings in cost and human resources.

The objective of this program is to study the feasibility of using ultrasonic acoustic signals and seismic impulses to rapidly predict the presence of large geological discontinuities or other potential sources of danger, such as old mine workings filled with water or gas, lying within a reasonable working range ahead of excavation surfaces. The principal geologic medium of interest is "hard" or crystalline rock.

The feasibility study indicated that the pulse-reflection technique is most suited to this application. With this method, reflecting interfaces in homogeneous rock have been detected. At a hard rock field test site which was weathered and extremely jointed with a destressed zone along the tunnel walls of the mine, various geological discontinuity interfaces could be identified with a reasonable level of confidence.

The results of this study go a long way toward proving the feasibility of this technique. However, further development work is needed to optimize an operating system in hard rock environments where excavation machines are used for tunneling.

DD FORM 1473

1a

14. KEY WORDS	LINK A		LINK B		LINK C	
	ROLE	WT	ROLE	WT	ROLE	WT
Rapid excavation system						
Geological Discontinuities						
Acoustic waves						
Pulse-reflection method						
Resonance method						
Cross-correlation						
Piezoelectric transducer						
Signal averaging						
Field experiments						
Acoustic Couplants						

SEISMIC DETERMINATION OF GEOLOGICAL DISCONTINUITIES AHEAD OF RAPID EXCAVATION

FINAL TECHNICAL RERORT

September 1972

Contract No: H0210033
Effectlve: April 30, 1971
Terminates: July 31, 1972
Amount: $87,062

Principal Investigator:
R. R. Gupta (313) 352-7740
Bendix Research Laboratories
Southfield, Michigan 48076

Project Engineer:
Charles F. Johnson

BRL Project 2412

TABLE OF CONTENTS

LIST OF ILLUSTRATIONS

SECTION 1
TECHNICAL REPORT SUMMARY

The purpose of this program is to determine the feasibility of using ultrasonic acoustic signals and seismic impulses to rapidly predict the presence of large geological discontinuities or other potential sources of danger, such as old mine workings filled with water or gas lying within a reasonable working range (a few feet to a few tens-of-feet) ahead of an excavation face. The principal geological medium of interest is "hard" or crystalline rock.

A review of existing literature and experimental data was made to determine the characteristics of hard or crystalline rocks, and other materials (that are most likely to be found near geological discontinuities of interest). This review indicated that at the ultrasonic frequencies of interest the energy of propagating sound waves in rock is attenuated predominantly by frictional losses. These frictional losses in rock increase exponentially as the product of the frequency and the distance traveled by the sound waves.

A theoretical study was made to investigate the feasibility of using several nondestructive ultrasonic techniques to detect the presence of a large geological discontinuity interface. The pulse-reflection (also called pulse-echo) method was found to be best suited to the proposed application.

A trade-off system study was undertaken to determine the optimum radiation frequency (or range of frequencies) most likely to delineate the geological discontinuities ahead of the excavation face. The results of this theoretical study showed that in a lossy rock medium, a moderate power pulse-echo detection system operating at about 30 kHz can detect large geological discontinuities up to six meters away from the excavation surface. In low-loss rocks, the maximum distances upto which a discontinuity can be seen is increased.

In order to couple sound energy into and out of rough surface rocks, an intermediary fluid acoustic medium (coupling medium) is needed to fill in spaces between a transducer and the rough surface of the rock. Theoretical and experimental studies were conducted to evaluate various coupling media that were compatible with the environment. Experimental results indicated that water, silicone oil, and glycerine have equal value as couplants. In applications where the rock surface is very rough and direct contact between the transducer housing and the rock surface does not result in adequate acoustic coupling, a noncontacting method of coupling may be used. This could be accomplished by maintaining a water jet (mixed with a wetting agent) between the transducer and the rock surface.

In the laboratory, reflecting interfaces in a homogeneous rock medium were detected using a pulse-reflection method. Based on these laboratory results and theoretical prediction from the trade-off study, field tests were planned and carried out at the Colorado School of Mines Experimental mine, a hard rock mine. The rock face at the field test site was weathered and extremely jointed with a destressed zone running along the mine walls which was caused by the use of explosives to excavate tunnels in the mine. The depth of the destressed zone varies from several inches to several feet. At this field site, various geological discontinuity interfaces could be identified with a reasonable level of confidence, using a cross-correlation method for signal processing.

In addition to the evaluation of the pulse-reflection method, preliminary theoretical/experimental investigations were carried out to determine if the sound generated by excavation machines could be advantageously used as a sound source for an acoustic detection technique. Resonance detection was judged to be the best approach using machine noise for the wide-band source of sound signal. In this approach, resonances are set up within the thickness of the rock medium bounded by the rock face and the discontinuity layer in the rock medium. A field experiment was designed where resonance detection was used; the acoustic source signals fed into the rock medium were generated by a

pneumatic drill machine boring into the rock face. The frequency spectrum analyses of the detected signals suggest the presence of a rock layer whose depth from the rock face varies anywhere from 1 foot to 2.5 feet. These results were found to be consistent with the pulse-reflection and refraction data. All these results agree with the known existence of the destressed zone in the tunnel walls of the mine. This preliminary field experiment using machine noise suggests that excavation machine noise may be used as a potential sound source for resonance detection of the first discontinuity layers up to several feet deep. However, it will be limited to cases where the discontinuity interface is parallel to the rock face and is therefore not a practical method.

The results of this study go an appreciable way toward proving the feasibility of using an acoustic pulse-reflection method to detect large geological discontinuities ahead of an excavation face. Further development work is needed to optimize an operating system in hard rock environments where excavation machines are used for tunneling.

The feasibility study has also led to a number of recommendations regarding the proposed detection system. The suggested prototype system will be based on a pulse-reflection technique and would have the following characteristics:

- FM pulse excitation of the transmitter, at frequencies from 5-15 kHz for detecting deep discontinuities (for example, 15-50 feet) which would give a resolution of about 3 feet, and 15-45 kHz for detecting shallow discontinuities (for example, 5-15 feet) which would give a resolution of about 1 foot

- The use of thickness-mode piezoelectric ceramic transducers, having resonant frequencies well above the highest operating frequency

- A directive source provided by a simple array

- A simple array of receivers to reduce the effect of undesired coherent signals via directivity

- A contained fluid to couple acoustic signals from transducer to rock face

- A cross-correlation method of signal processing with the modified transmitter excitation pulse. This modification of the input pulse will compensate for the effects of the transducer, coupling medium, and the signal amplitude attenuation due to frictional losses in the rock medium.

SECTION 2
INTRODUCTION

A method of probing the geologic medium ahead of continuous excavation machines, in real-time, is essential to avoid, or be prepared for, hazardous or difficult formations. Knowledge of potential hazards will result in increased safety for both man and equipment, and will allow excavation to proceed at the maximum speed.

For the next generation excavation equipment, the rate-of-advance has been projected to be about 200 feet per day. Thus it would be very desirable to have a detection system that could predict the presence of geological anomalies within a working range of about 200 feet in advance of the excavation machine. Unfortunately, a detection system capable of predicting anomalies in hard rock that far away with a <u>reasonable level of confidence</u> is beyond the existing technology. However, with existing acoustic technology, the detection of geological anomalies in real time within a working range of a few tens-of-feet in hard rock appears feasible with a reasonable level of confidence. Bendix Research Laboratories feel that a detection system based on this range is adequate for the proposed application, provided that the range data are periodically updated by probing the excavation face every few feet. In a sense, the data from successive measurements would be stacked to improve detection. At present, we do not know what the next generation machines will look like, but if they are similar to those used today, the transmitting and receiving probes could be retractable devices mounted on the cutting head of the machine. The time scale implied by "real time" is of the order of few minutes, which is made up of the instrument preparation time, measurement time, processing and display times. The periodic sampling of the excavation face at every few feet could be carried out at each tunneling machine stop, when the body of the machine is being advanced for the next tunneling operation while the cutting head is stationary. Because of

continuous updating of anomaly range data within the prediction range, the confidence level in the stacked acoustic detection procedure is expected to be greater than one where anomalies are detected over a range of a few hundred feet by a single probing of the excavation face.

The objective of this program is to study the feasibility of using ultrasonic acoustic signals and seismic impulses to rapidly predict the presence of large geological discontinuities or other potential sources of danger, such as old mine workings filled with water or gas, lying within a reasonable working range (a few feet to a few tens-of-feet) ahead of an excavation face. The principal geologic medium of interest is "hard" or crystalline rock.

The goal of the program is to recommend a practical detection system capable of identifying significant geological anomalies ahead of excavation face.

Section 3 presents the technical discussion of the proposed detection system. Basic principles underlying the design and development of a pulse-reflection system are reviewed in Section 4, and experimental laboratory investigations are described in Section 5. Section 6 presents results of a field test carried out to show feasibility of the acoustic techniques. Signal processing techniques applicable to the field data are also reviewed in Section 6, along with interpretation of the processed field data. Section 7 presents the conclusions of this phase and recommendations for the next phase of the program.

SECTION 3
TECHNICAL DISCUSSION

3.1 GENERAL

The distance to which the presence of an anomaly or a discontinuity in a geologic medium can be detected depends on such parameters as the characteristics of the rock medium, the type of anomaly, and the probing frequency. It was proposed that the acoustic detection system be capable of locating a geologic anomaly interface which is at least as large as the excavation face. The lateral dimensions of such an anomaly are assumed to be larger than the probing signal wavelength.

At the signal wavelengths of interest, the rock medium ahead of an excavation face would appear semi-infinite in extent to the acoustic waves propagating through it. In such a solid medium, longitudinal, shear and Rayleigh waves can be excited. The longitudinal and shear waves (body waves) can propagate throughout a solid medium whereas Rayleigh waves propagate only over the free surface of such a medium. Longitudinal waves travel the fastest, while the Rayleigh waves travel the slowest.

Many rock formations contain cracks and fracture zones which may be filled with water or gas. Shear waves can not propagate through these fluid-filled zones whereas longitudinal waves can. Therefore, the proposed system will be based on the detection of longitudinal waves.

In an ideal propagation medium, sound pressure decreases inversely with the distance from the source due to geometrical spreading of the wave. In natural solid materials, sound pressure is further weakened by scattering of the signal and by frictional losses. In a hard rock medium, scattering losses only become significant at signal frequencies in the megahertz region where the grain size is as large as the signal wavelength. In the proposed application, the frequencies of interest are in the low kilohertz region where the signal amplitude would be

attenuated predominantly by frictional losses in the rock medium. These frictional losses depend on such factors as pressure, porosity, degree of water saturation, grain size, and the types of propagating waves. The attenuation of the signal is commonly approximated by

$$\exp(-\alpha L) \tag{1}$$

where L is the total distance traveled, and α is the attenuation constant of the rock medium. The constant α is known to vary linearly with the signal frequency which makes the quality factor Q of a rock essentially independent of signal frequency. Q is defined as $\pi f/\alpha v$. A majority of hard rocks are reported to have their Q value somewhere between 20 to 200.[1,2]

In a geologic medium, the presence of an anomaly or a discontinuity interface is characterized by a sudden change in the acoustic impedance of the medium at this interface. Acoustic impedance Z is given by the product of the density ρ and the sound velocity v in the medium; i.e.,

$$Z = \rho v \tag{2}$$

The percentage of the signal reflected back by a discontinuity interface depends on the acoustic impedance contrast at the interface. The higher the impedance contrast at the interface, the higher the signal reflected back by the anomaly.

3.2 EVALUATION OF DETECTION TECHNIQUES

The feasibility of several ultrasonic techniques for detecting large geologic anomalies in hard rock was investigated. The acoustic phenomena analyzed in this study were: (1) pulse reflection, (2) resonance, (3) changes in the scattering characteristics of the return signal, and (4) phase of the continuous waves.

The pulse-reflection (also called pulse-echo) technique was found to be most suited to the proposed application. This technique uses well-defined acoustic signals which are commonly generated by using either piezoelectric ceramic or magnetorestrictive transducer elements. On the other hand, it would be highly desirable if a detection approach can be found, that can use, advantageously, the ever present sound waves generated by excavation machines. The wide band frequency spectrum of such machine noise makes it suitable as a source for a resonance detection technique. However resonance detection is limited to applications where the discontinuity interface is parallel to the excavation face.

Methods using changes in scattering properties and phase detection of continuous waves were found unsuitable for this application.

A detailed discussion of the detection techniques was presented in the semiannual technical report.[3] For completeness, we will however review both pulse-reflection and resonance phenomena.

3.2.1 Pulse Reflection

Pulse reflection is a well established technique for non-destructively measuring the thickness of a testing material or detecting its internal flaws. The basis of this method is to transmit a burst of acoustic signal into a test material; when the transmitted pulse encounters a reflecting interface (i.e., an impedance mismatch interface), an echo is reflected back towards the receiving transducer. The transit time t of the pulse from the transmitter to the discontinuity and back to the receiver can be used to determine the thickness L of a test material or the distance to a flaw by

$$L = \frac{vt}{2}$$

(3)

provided the sound velocity v in the test material is known.

The relative amount of signal reflected by a discontinuity interface depends on the angle of incidence of the waves and on the

relative impedance mismatch at the discontinuity. Whenever a sound beam is incident other than normally to a discontinuity interface (between two solid materials with different sound velocities), mode-conversion to other types of waves may occur. In this case, energy is carried by both reflected and refracted longitudinal and shear sound beams which are generated by mode-conversion. If the angle of incidence of the longitudinal sound waves exceeds the critical angle for the production of refracted shear waves, refracted shear waves cannot be produced. However, yet another waveform, known as Rayleigh waves, can be produced which propagates at the free surface of a solid material.

At normal incidence, the ratio of the reflected energy W_r to the incident energy W_i is given by the reflection coefficient R,

$$R = \frac{W_r}{W_i} = \left(\frac{Z_2 - Z_1}{Z_2 + Z_1} \right)^2 = \left(\frac{\rho_2 v_2 - \rho_1 v_1}{\rho_2 v_2 + \rho_1 v_1} \right)^2 \tag{4}$$

and the transmission coefficient T is given by

$$T = (1 - R) = \left(\frac{2 Z_2}{Z_1 + Z_2} \right)^2 = \left(\frac{2 \rho_2 v_2}{\rho_2 v_2 - \rho_1 v_1} \right)^2 \tag{5}$$

where ρ, v, and Z, respectively, are the density, sound velocity, and impedance of the medium. The subscripts 1 and 2 refer to the media in front of and behind the discontinuity, respectively.

In a pulse-reflection system, the minimum depth of a discontinuity interface that can be measured is limited by the pulse

width of the radiated pulse, whereas the maximum depth is limited by the frictional and scattering losses in the rock medium. A pulse-reflection system is preferred over other systems because it requires relatively low average power while the peak power transmitted is high enough to operate at a favorable signal-to-noise ratio. Furthermore, it is relatively simple, in this case, to discriminate in the time domain against some of the undesired coherent signals (which may be direct surface waves or reflected surface waves).

3.2.2 Resonance

The resonance technique is commonly used for measuring material thickness, especially that of metals. This method is applicable when the transverse dimensions of a specimen are large compared to both the probing wavelength and the thickness of the plate.

In the resonance method, standing waves are set up within the test material whenever its thickness is an integral multiple of one-half of the signal wavelength. The resonance can be detected by the loading effects upon the transmitting or receiving transducer. The thickness L of a test material is given by

$$L = \frac{n\lambda}{2} = \frac{nv}{2f} \qquad (6)$$

where λ is the wavelength in the test material and v is the sound phase velocity in the test material, f is the resonance frequency of the fundamental mode in the plate, and n is the integral number of half-wavelengths set up in the test material.

SECTION 4

PULSE-REFLECTION SYSTEM DESIGN

In this section, the basic principles underlying the design, development, and testing of a pulse-reflection technique are briefly discussed. The effects of various parameters of the detection system are also analyzed in a system trade-off study.

4.1 GENERATION AND RECEPTION OF ACOUSTIC SIGNALS

The acoustic signal, in general, can be generated by a mechanical source or an electromechanical transducer. A mechanical source (such as a mechanical impactor or explosive charge) was found unsuitable because the frequency spectrum of such a source can not as easily be controlled to transmit a desired acoustic waveform. On the other hand, electromechanical transducers are well suited to this application and were therefore selected for further investigation. Such devices can be used either as transmitters or as receivers since they transform mechanical energy into electrical energy, and vice versa.

4.1.1 Transducer Material

At operating frequencies of interest (which lie in the kilohertz region), piezoelectric ceramic transducers are preferred over magnetorestrictive ones due to the former's low cost, smaller size, and higher efficiency. Quartz, and cast ceramic materials (such as lithium sulphate, barium titanate, lead meta-niobate, and lead zirconate-titanate base materials) are commonly used piezoelectric materials. Except for the fact that quartz is stronger and is a lower-loss material, ceramics are more efficient and lower in cost. Furthermore, ceramics can be readily processed into larger or more complex shapes, and they require a much lower driving voltage.

Two piezoelectric coefficients, d and g, are important in evaluating a transducer material. The constant d measures either the amount of charge produced on the electrodes attached to a piezoelectric crystal which is subjected to a given force or the deflection caused by a particular applied voltage. The g constant is used to denote the field produced in a piezoelectric crystal by an applied stress. The constants d and g are interrelated by the dielectric constant $\epsilon_o \epsilon_r$ of the material by

$$g = \frac{d}{\epsilon_r \epsilon_o} \qquad (7)$$

where ϵ_o is the permittivity of vacuum. A piezoelectric material with a large value of d is desirable for a transmitter, while the material with a large value of g is useful for a receiver. Essentially d and g should both be high in order to obtain optimum transfer of mechanical energy into electrical energy or vice versa. This is evident from the fact that the electromechanical coefficient k_c^2 is related to g, d, and Young's modulus c by the following relationship

$$k_c^2 = gdc = e^2/\epsilon_r \epsilon_o c \qquad (8)$$

where e is the piezoelectric stress constant.

4.1.2 Transmitter Material

The physical constants of several commonly used transducer materials are listed in Table 4-1. Both PZT-4 (lead zirconate-titanate base) ceramic and LMN (lead meta-niobate) appear to be well suited as transmitter materials.   A PZT-4 transmitter is preferred over LMN for the former's high power capabilities (due to high resistance to depolarization and low dielectric losses under high electric drive), high electromechanical coupling coefficient, and high Curie point.

Table 4-1 – Constants of Various Piezoelectric Materials

Physical Property	Quartz 0° X-cut	Lithium Sulfate 0° Y-cut	Barium Titanate Type B	Lead Zirconate-Titanate		Lead Meta-Niobate	Units
				PZT-4*	PZT-5*		
Density ρ	2.65	2.06	5.6	7.6	7.7	5.8	10^3 kg/m^3
Acoustic impedance ρc	15.2	11.2	24	30.0	28.0	16	10^6 kg/m^2 S
Maximum operating temperature	550	75	70-90	250	290	500	°C
Dielectric constant	4.5	10.3	1,700	1,300	1,700	225	---
Electromechanical coupling factor for thickness mode k_{33}	0.1	0.35	0.48	0.64	0.675	0.42	---
Electromechanical coupling factor for radial mode k_r	0.1	---	0.33	0.58	0.60	0.07	---
Elastic quality factor Q	10^6	---	400	500	75	11	---
Piezoelectric modulus for thickness mode d_{33}	2.3	16	149	285	374	85	10^{-12} m/V
Piezoelectric pressure constant g_{33}	58	175	14.0	26.1	24.8	42.5	10^{-3} V/m/(N/m^2)
Volume resistivity at 25°C	$>10^{12}$	---	$>10^{11}$	$>10^{12}$	$>10^{13}$	10^9	---
Curie temperature	575	---	115	320	365	550	°C
Young's modulus E	8.0	---	11.8	8.15	6.75	2.9	10^{10} N/m^2
Rated dynamic tensile strength	---	---	---	3,500	4,000	---	psi

*PZT – It is a trademark of the Clevite Corporation.

LMN has the advantage over PZT-4 of relatively low transient response which is due to relatively high dielectric losses. No vendor was found who could provide LMN in the desired shape and size needed for fabricating a transmitter. Consequently, PZT-4 was selected for the design and fabrication of transmitters.

4.1.3 Transmittere Excitation Waveforms

In a pulse-reflection system, the minimum depth of a discontinuity that can be measured is limited by the fact that the travel time of the echo should be longer than the duration of the radiated pulse. Therefore, it is highly desirable to radiate as narrow an acoustic signal pulse as practical. The acoustic signal radiated into a rock medium is made of forced oscillations (which are caused by the excitation waveform) and the transient (i.e., buildup and decay) oscillations of the loaded transducer. The forced response waveform is similar to the excitation waveform, whereas the dominant signals in the transient response are at those transducer resonant frequencies which are in the neighborhood of the excitation frequencies.

Some method of signal processing is needed to identify the desired reflected signals contained in the total received signal. Both cross-correlation and time-averaging methods of signal enhancement appear to be most useful for this purpose and are discussed in Section 6. For effective signal processing, it is desired that the actual radiated signal closely resemble the excitation wavefore or that the correlation form is the same as the radiated signal. This can, in principle, be achieved by highly damping the transient oscillations of the transducer and by operating at frequencies away from the resonant frequencies of the transmitter.

Although, in principle, any electrical waveform can be used to excite a piezoelectric transmitter, the most suitable electrical excitation waveforms are

- Signal sinusoidal cycle signals
- Pulse-modulated continuous waves (PM-CW) signal
- Frequency-modulated (FM) pulse signals

These waveforms were experimentally evaluated in the laboratory and field tests.

4.1.4 Receiver Material

The transient behavior of a receiving transducer distorts the original shape of the pulse signal arriving at the transducer. This distortion of the pulse can be reduced to a great extent by using a highly damped receiver and by operating at frequencies below the lowest resonant frequency of the receiver.

Lithium sulphate, LMN, and PZT ceramics are well suited receiver materials. Lithium sulphate is, however, limited to temperatures below 75 degrees because it decomposes at about 110°C. PZT ceramics (such as PZT-4 and PZT-5) have higher dielectric constants and hence higher impedance than LMN, and therefore the loss in signal strength due to impedance loading of connecting cables will be relatively small. Receivers were made out of both PZT and LMN, and their relative performance was experimentally evaluated. Although PZT receivers distorted the received signal more than LMN (due to relatively long transient response), PZT receivers were used in the field tests because of their higher sensitivity.

4.2 ACOUSTIC COUPLING MEDIA

In order to couple acoustic energy from transducer to rock and vice versa, an intermediary coupling medium is required to fill in uneven spaces and provide intimate acoustic coupling from a transducer to a rock surface. In principle, a couplant can be almost any material, solid or liquid, which

- Is compatible with the tunneling operation
- Wets both the rock surface and the face of the transducer probe
- Is easily contained
- Is homogeneous and free from bubbles or solid particles which reflect or scatter the incident beam

- Is not corrosive, toxic, or flammable
- Has an acoustic impedance approaching that of bounding media (this is an ideal rather than a restrictive requirement).

4.2.1 Transmission Through a Coupling Layer

The thickness of a couplant layer will affect the acoustic impedance of a coupling medium if the transit time of the incident mono-frequency pulse through the coupling layer is less than the duration of the incident pulse. In this case, the propagating pulse experiences interference similar to that of continuous waves. The general expression for the energy transmission coefficient T_{13} for a plane sound wave, incident normal to a pair of smooth parallel interfaces, is given by[5]

$$T_{13} = \frac{4\,\rho_3\,v_3\,\rho_1\,v_1}{(\rho_3\,v_3 + \rho_1\,v_1)^2 \cos^2 k_2\,L + (\rho_2\,v_2 + \rho_3\,v_3\,\rho_1\,v_1/\rho_2\,v_2)^2 \sin^2 k_2\,L} \tag{9}$$

where ρ and v are, respectively, the density and sound velocity of the media. Subscripts 1, 2, 3 refer respectively to the transducer, coupling medium, and radiation medium. L is the thickness of the coupling layer, and $k_2 = 2\pi/\lambda_2$ where λ_2 is the sound wavelength in the coupling medium.

If the acoustic impedance of a couplant is intermediate between those of the bounding media, transmission through the couplant is maximum when its thickness is an odd multiple of a quarter wavelength. If, in addition, the acoustic impedance of the couplant is equal to the geometric mean of the impedances of the bounding media, there is complete transmission. If, however, the acoustic impedance of the coupling layer is not intermediate between those of the bounding media, then the transmission is maximum (i.e., T_{13} approaches T_{12}) when the thickness of the layer approaches zero or a multiple of one-half of the signal wavelength. The transmission becomes minimum when the thickness is an odd multiple

cf a quarter wavelength. For coupling layer thicknesses smaller than a quarter wavelength, the transmission is less than it would be without the couplant, and the transmission decreases with increasing thickness of the coupling layer.

If the duration of the incident signal pulse is short compared to the transit time through the couplant, a given incident pulse splits into a series of reflected and transmitted pulses, completely separated and mutually independent. The relative amplitude of the these pulses can be calculated according to equations (4) and (5) if these equations are repeatedly applied to the individual reflection and transmission phenomena. As a result of repeated splitting, the amplitude of the transmitted pulse sequence then decreases continuously, but remains fairly independent of the thickness of the coupling layer. This case was not encountered in this work however.

4.2.2 Surface Roughness

When plane longitudinal waves are incident upon a rough surface, they enter at various angles with respect to the normal at various points on the rough surface. When the angle of incidence exceeds the critical angle for a certain mode of propagation within the rock material, these waves are not transmitted, and mode-conversion to shear and surface waves results. Thus, a portion of the beam is interrupted in transmission across a rough surface rock.

There are certain degrees of surface roughness that can produce phase cancellation in the transmitted wave, even with normal incidence. The sound that travels through a fluid couplant lags the sound which travels through a rock because sound velocity in a coupling fluid is lower than that in a typical rock. The sound recombines inside the rock so as to accommodate the difference in travel time. When this difference in travel time (resulting from different couplant thicknesses between the transducer face and rough surface rock) is equal to one-half the period of sound wave, a pressure wave combines with a rarefaction wave, and the resultant energy is nearly zero inside the rock. The average

peak-to-valley roughness that causes the destructive interference is known as the critical roughness and is given by[6]

$$R_c = \frac{\lambda_2 \, v_1}{2(v_2 - v_1)} = \frac{\lambda_1 \, v_2}{2(v_2 - v_1)} \qquad (10)$$

where λ_1 and λ_2 are the wavelengths of sound in the couplant and rock, respectively; and v_1 and v_2, respectively, are the velocities of the sound in the couplant and rock. There are similar destructive interferences for roughness values of $2R_c$, $3R_c$, etc. In a practical application, the peak-to-valley surface roughness should therefore be much smaller than the critical roughness given by equation (7); the surface effects are usually insignificant when the peak-to-valley roughness is less than 1/8 of the wavelength in the coupling medium.

4.3 TRANSMITTER-RECEIVER TRANSDUCERS CONFIGURATIONS

The interface of a geological discontinuity is not normally parallel to the excavation face but rather at an angle to it. The selected transmitter-receiver arrangement must be able to detect such an inclined interface. The simplest and most economical arrangement would be to use a single transmitting probe in the center of the excavation face and three spatially separated receiving probes. The travel time of the reflected signals would give the depth of a discontinuity interface, whereas the difference in travel times would provide the inclination of the discontinuity interface. The transmitting and receiving transducers in general must be spaced such that the desired reflected signals arrive either before the arrival or after the departure of undesired signals (such as surface waves) propagating over the excavation face.

In addition to this simple arrangement of transducers, two other suitable arrangements of transducers were evaluated for their relative detection effectiveness. These arrangements were:

- Four common transmit-receive (TR) transducer probes
- One transmitting transducer and multiple receiving transducers

(In the BRL proposal, one more arrangement using one transmitter and a receiving phased-array was proposed which is a special case of the arrangement using multiple receiving transducers and therefore is not enumerated separately.)

In TR transducer probe, a single transducer is used with common connections to the transmitter and receiver amplifier unit. In this case, the signals that are amplified by the receiving amplifier fall into two categories: (1) the signals that are scattered or reflected back by the rock medium and (2) the internally reflected signals that are due to multiple reflections of the transmitted waveform within the transducer. In lossy rock applications, these internally reflected signals can be quite large relative to the desired signals that are reflected back, especially from deep discontinuities, and consequently identification of discontinuities becomes difficult. Furthermore, each TR probe in a multiple TR probe configuration needs a separate high-voltage protection. The advantage of a TR probe is essentially fewer transducers; however, this is achieved at the expense of increased system complexity. These practical considerations make the use of a TR probe less attractive for the proposed application than configurations using separate transmitters and receivers.

The remaining two transducer configurations differ only in the arrangement of receiving transducers. A series of receiving transducers (a receiving array) is commonly used in sonar for either discriminating via directivity against undesired coherent sources present in a uniform medium and/or scanning for targets over a large volume by steering the narrow beam of the receiver array. We have evaluated the usage of such sonar arrays as DIMUS[8-9] and DICANNE[10] which are useful in a homogeneous medium. Most hard rock media of interest are full of fractures and joints; in addition, the rock face is expected to be relatively rough.

These characteristics make the rock medium look nonuniform to a receiving array. In such an inhomogeneous medium, the effectiveness of these arrays is dubious, especially in the presence of multiple undesired sources of coherent signals. In addition, the array size is constrained by the fact that (a) it must be compatible for mounting on an excavation machine (or surface) and (b) there must be uniform acoustic coupling of the receivers to the rock surface which is usually relatively rough. These considerations suggest the use of a simple array with as few receivers as possible. Therefore, the simple arrangment of one transmitter and three receivers has been selected for field tests.

4.4 OPERATING FREQUENCY SELECTION

A trade-off system study was made to determine the optimum radiation frequency (or range of frequencies) most likely to delineate a large discontinuity in "hard" crystalline rock media.

The effect of frequency on detection range was explored using theoretical calculations for a pulse-modulated continuous wave system operating in a hard rock medium. In these calculations it is assumed that:

- The discontinuity interface is at least as large as the excavation face
- The transmitter is a half-wavelength thick (Longevin-type) cylindrical sandwich transducer
- The beam width of the transmitter is broad enough to illuminate the nearest significant discontinuity interface of interest
- The signals are attenuated primarily by the frictional losses in rock
- The reflected signal is detected by a nonresonant receiver
- The transmitting and receiving transducers are so located that the desired reflected signals appear at the receiver after surface waves have departed from it.

The derivation of the range-frequency relationship is presented in Appendix A. The results are depicted in Figure 4-1, where the upper curve is calculated for a low-loss granite rock of Q = 125. The lower curve is for a high-loss rock of Q = 20. These curves show that at a frequency of 30 kHz, an air-backed granite interface in a high-loss granite can be detected up to 6 meters, whereas the same discontinuity
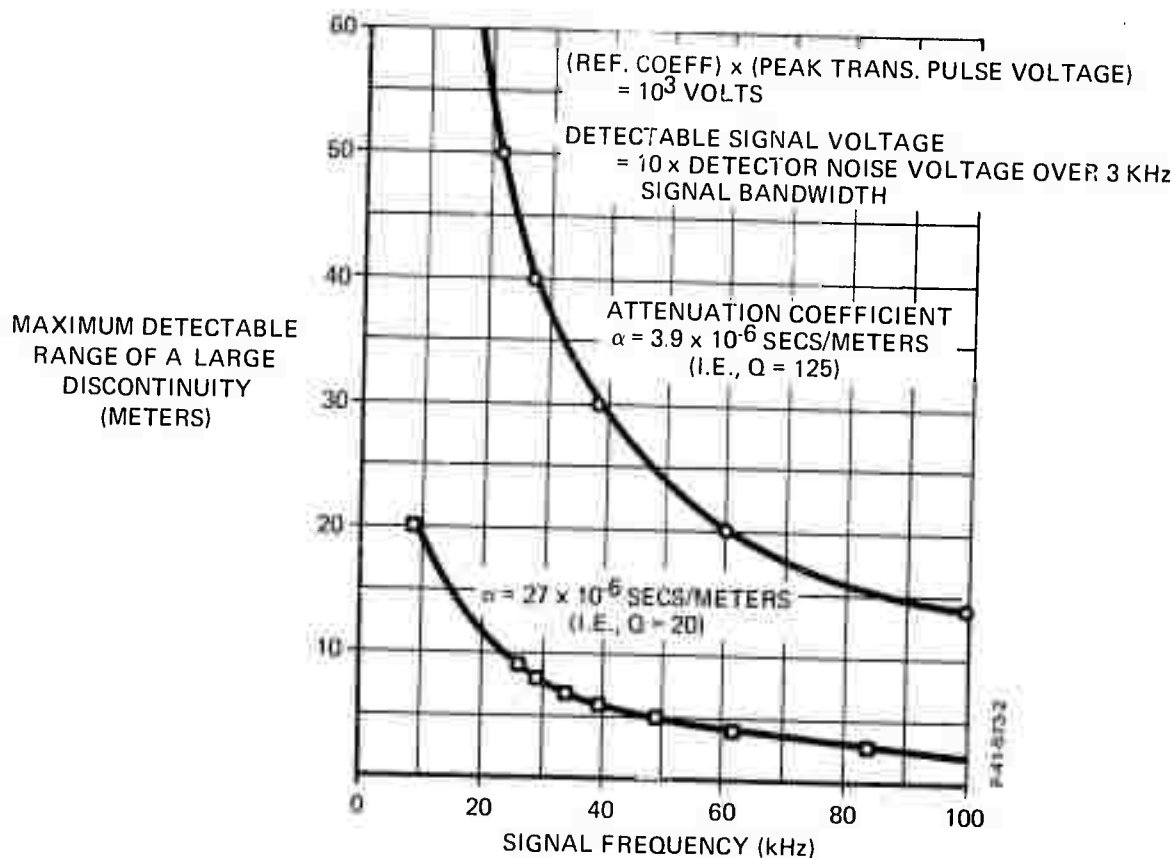
ASSUMPTIONS

PULSE WIDTH: 300 μsec
REPETITION FREQUENCY: 20 Hz
TRANSMITTER: LANGEVIN CYLINDRICAL SANDWICH
            TRANSDUCER (4″ DIAMETER, λ/2 THICKNESS)
RECEIVER: NON-RESONANT
            (2″ DIAMETER - ½″ THICK)
TRANSDUCTION EFFICIENCY: 2.5 PERCENT
PEAK EXCITATION VOLTAGE: 1000V
INTERFACE: GRANITE-AIR

Figure 4-1 – Theoretical Range-Frequency Curves for a Pulse-Modulated CW System Operating in Granite Rock

can be easily seen up to 35 meters in a low-loss granite. Based on
these calculations and the desired maximum depth of penetration (a few
tens-of-feet), the radiation frequency in the neighborhood of 30 kHz
was chosen for further experimental investigation.

SECTION 5
LABORATORY EXPERIMENTAL INVESTIGATIONS

In order to establish the validity of the chosen ultrasonic pulse-reflection technique, preliminary laboratory and field experiments were designed to give information on the coupling of acoustic energy into and out of smooth as well as rough surface "hard" or crystalline rocks, and on the reflection from known hard rock structures of reasonable size.

5.1   HARD CRYSTALLINE ROCK TEST SPECIMENS

The test frequencies of interest are in the neighborhood of 30 kHz and hence the test wavelength in granite would typically be 7 inches. It is desirable to have test specimens whose dimensions are such that they appear laterally as semi-infinite media at the test wavelengths. However, considerations of availability, handling, and cost resulted in using a fine grain smooth surface hard granite block (of size 1' x 4' x 12') for reflection studies, and in the procurement of a hard red, coarse grain, granite block (of size 8" x 29" x 37") for coupling studies. The red granite block has both polished and rough (rock-pitch) finished surfaces.   The average peak-to-valley roughness of the rock surface is about 3/4".

5.2   FABRICATION OF TRANSMITTING AND RECEIVING TRANSDUCERS

A transducer can be made to operate in a resonant or a nonresonant mode.   In the resonant mode, the transducer operates at one of its resonant frequencies; whereas in a nonresonant mode, the transducer operates off-resonance, usually below its lowest resonant frequency. The electro-acoustic efficiency of a transducer increases as the operating frequency approaches any one of the resonant frequencies.   Transducer operation at resonance generates a relatively long transient response which makes it unsuitable in certain applications.

The transmitting transducers were designed to operate as resonant transducers because of high electro-acoustic conversion efficiency. These were half-wavelength thick (Langevin-type[11]) sandwich transducers which used PZT-4 annular discs.

For the reason of high acousto-electric conversion efficiency, a few of the receiving transducers were designed to operate as nonresonant transducers; these were also Longevin-type sandwiches.

To obtain a highly directive, narrow beam, transducers having a large ratio of transducer face diameter D to the signal wavelength λ should be used. However, because transducers of this geometry are not readily available, five resonant-mode transducers having D/λ less than unity were designed and constructed. The receiving transducers are cylindrical in shape having a D/λ of about 2/7. One of the transmitting transducers is similar to the receiving transducer except the front plate was tapered out so that it gave a D/λ of about 4/7. The other transmitting transducer is identical to the receivers except that it has a D/λ of about 5/7. A sketch of the sandwich transducer is shown in Figure 5-1.

These unloaded sandwich transducers were observed to resonate at the designed (thickness-mode) resonant frequency of 33 kHz. However, in addition, they were observed to resonate at about 23 kHz. This lower resonant frequency is not clearly related to either the thickness or the diameter of the cylindrical sandwich. A typical resonance spectrum of an unloaded 5-inch diameter transducer is shown in Figure 5-2. The next highest resonance after 33 kHz was observed to be at about 43 kHz. (In these figures, some of the resonance peaks above 80 kHz may be due to the receiver resonances.) The quality factor of the unloaded sandwich transducers is calculated to be about 20.

In addition to resonant receivers, several nonresonant (planar disc) receiving transducers were fabricated from PZT and LMN.

Also, two different types of commercially available receiving transducers were evaluated. These were: (a) high-Q (> 20) 90 kHz resonant frequency, 1-inch diameter cylindrical transducer (Model S-141B, Dungan
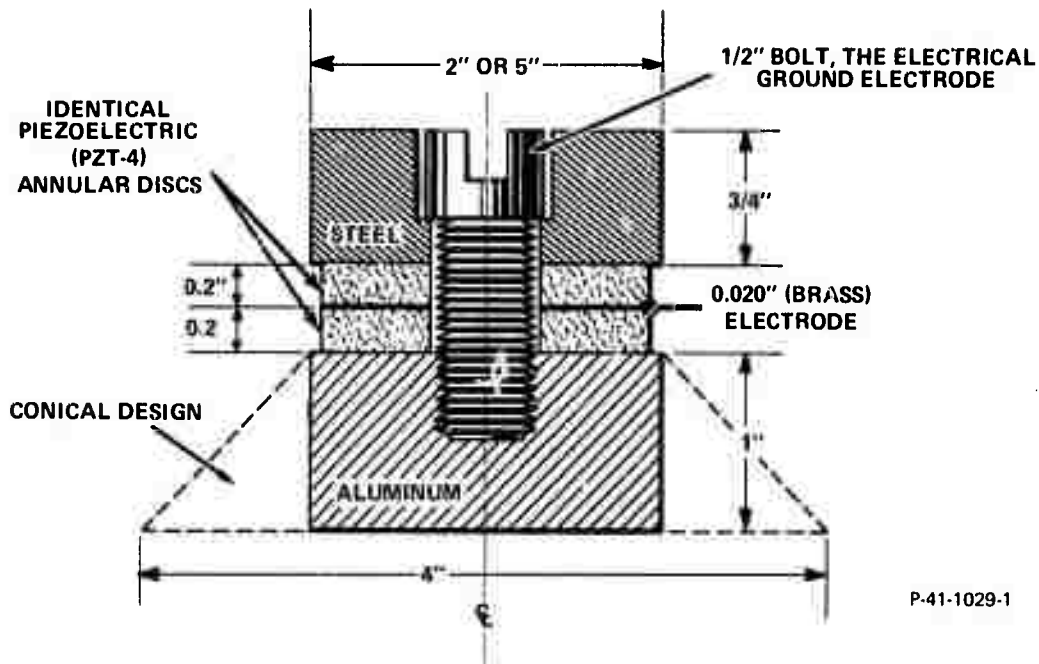
Figure 5-1 - Cylindrical Sandwich Transducer 5 Inches in Diameter
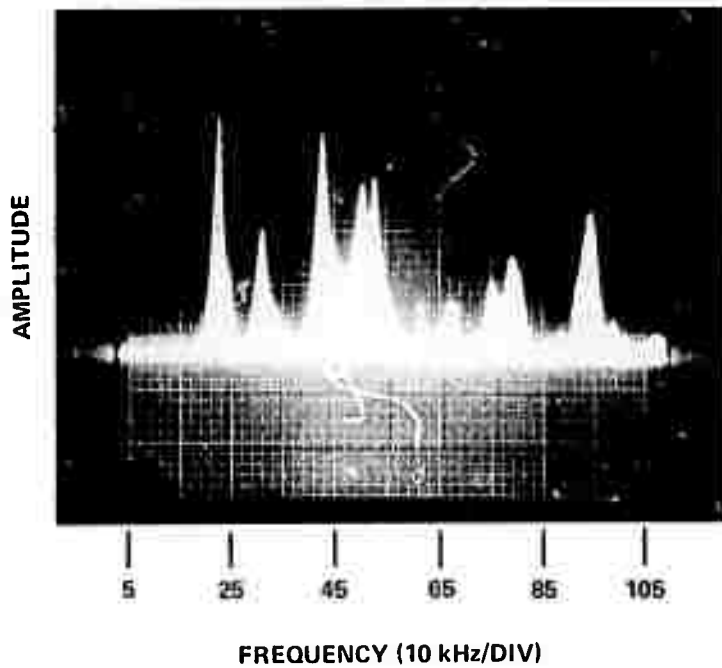
Figure 5-2 - Resonance Spectrum of 5-Inch Diameter
Cylindrical Sandwich Transducer

Research Corporation), and (b) low-Q (~ 4), 112 kHz resonant frequency, 1-1/2-inch diameter cylindrical transducer (Model J-302, Automation Industries). Low-Q transducers were also used as transmitting transducers.

5.3 EVALUATION OF EXCITATION SOURCES

Three appropriate pulse-excitation source setups were experimentally evaluated. These were:

(1) Narrow (several microseconds duration) high-voltage impulses (up to 1600 V peak open-circuit voltage) generated by a James Electronic Impulse Generator. This generator had a high output impedance and resulted in persistent electrical transient ringing across the transducer which in turn yielded an extremely long acoustic pulse.

(2) A PM-CW signal was obtained by gating the signal from a General Radio Audio frequency generator. The output of the gate was amplified by a Dynakit Mark III before being applied to the transducer. Again, in this case, persistent electrical ringing was observed across the transducer which resulted in a very long duration acoustic pulse.

(3) A function generator- (low output impedance) amplifier combination. The function generator is the model F-34, manufactured by Interstate Electronics Corporation. The output impedance of the function generator is 50 ohms and it is capable of generating (up to 10 volts peak) single sinusoidal cycles, PM-CW, FM and rectangular pulse signals. The output of this function generator is amplified by a 6 ohms output-impedance Krohn-Hite amplifier having a voltage gain of 10.

The last setup, in comparison to the first two, gave the least amount of transient electrical oscillations across the transmitter and, consequently, resulted in the least distorted radiated acoustic pulse. This setup was used for most of the experimental work.

5.4 COUPLING STUDIES

Consistent with the theoretical discussion presented in Section 4.2 we have selected (1) water (mixed with a wetting agent), (2) glycerine, (3) silicone, (4) greased neoprene, (5) J. E. Coupling paste (supplied by James Electronics, Incorporated), and (6) Dow Corning's Sylgard 51 gel as couplant candidates for experimental evaluation. These couplants were experimentally evaluated by carrying out transmission tests through a 29-inch thickness of the rock specimen. The experimental setup is shown in Figure 5-3. Transmission tests were conducted at about 33 kHz by coupling energy through smooth as well as rough rock surfaces. At the test frequency, the average roughness of the test specimen was about 1/8 of the signal wavelength. These couplants were evaluated as a function of their thickness, which in most cases was gradually increased up to a wavelength in the coupling medium.

Despite the fact that steady-state (relative to the duration of transmitted wave train) conditions existed for the behavior of couplants, only the transient response of a couplant (i.e., the first couple of cycles of the leading edge of the signal transmitted through a couplant) could be clearly identified, due to interference caused by the multiple reflections within the experimental rock block. Figures 5-4 and 5-5 show the transmitted signal through 29 inches of the test rock specimen
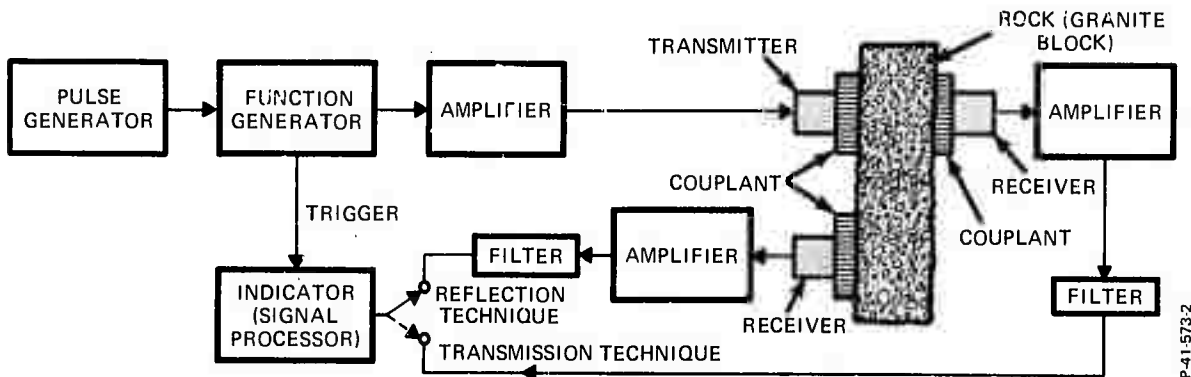
Figure 5-3 - Schematic Diagram of Pulse-Reflection (or Pulse-Transmission) Detection System
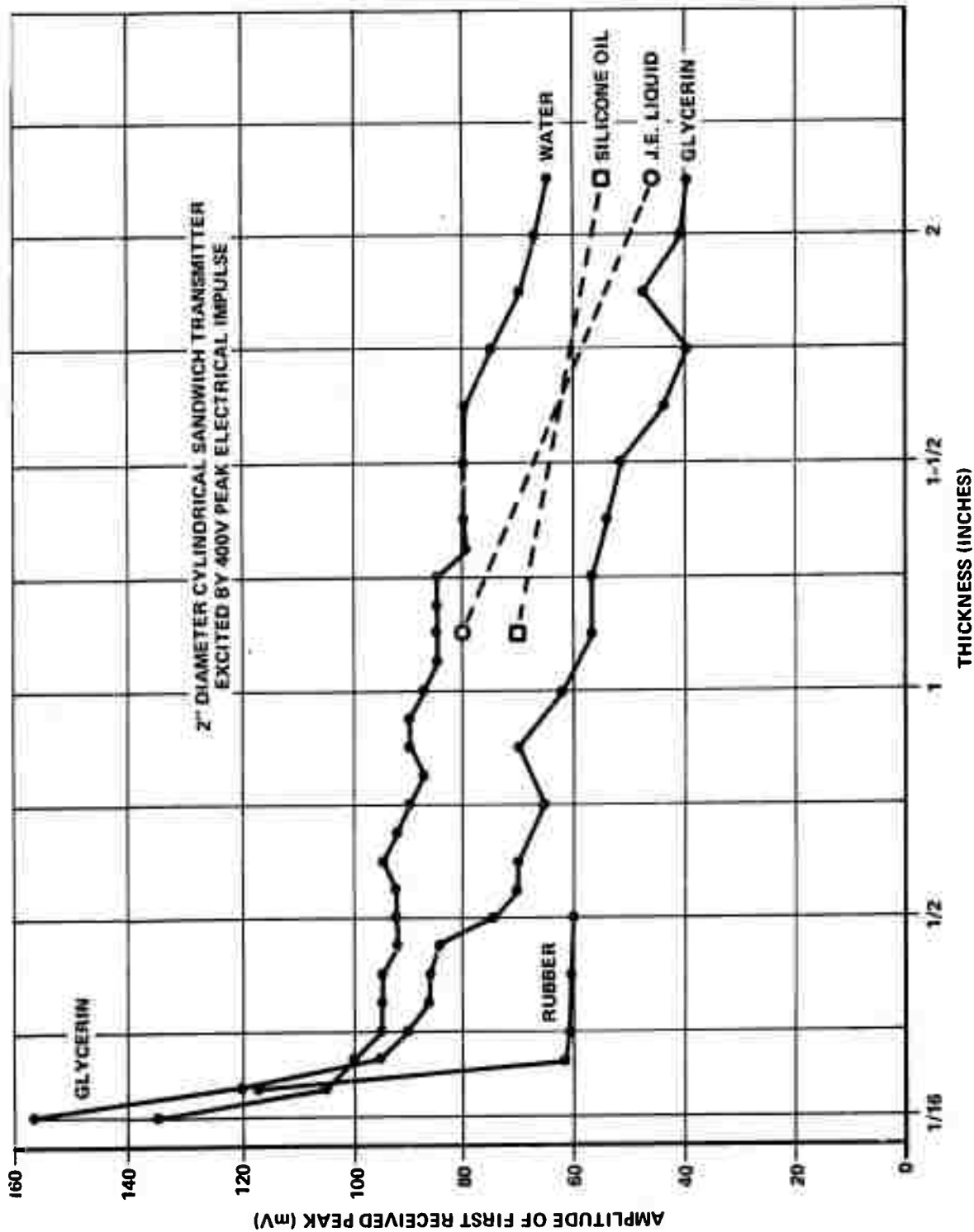
Figure 5-4 - Relative Transmission of Various Coupling Materials
Through 29-Inch Red Granite Having Smooth Surface
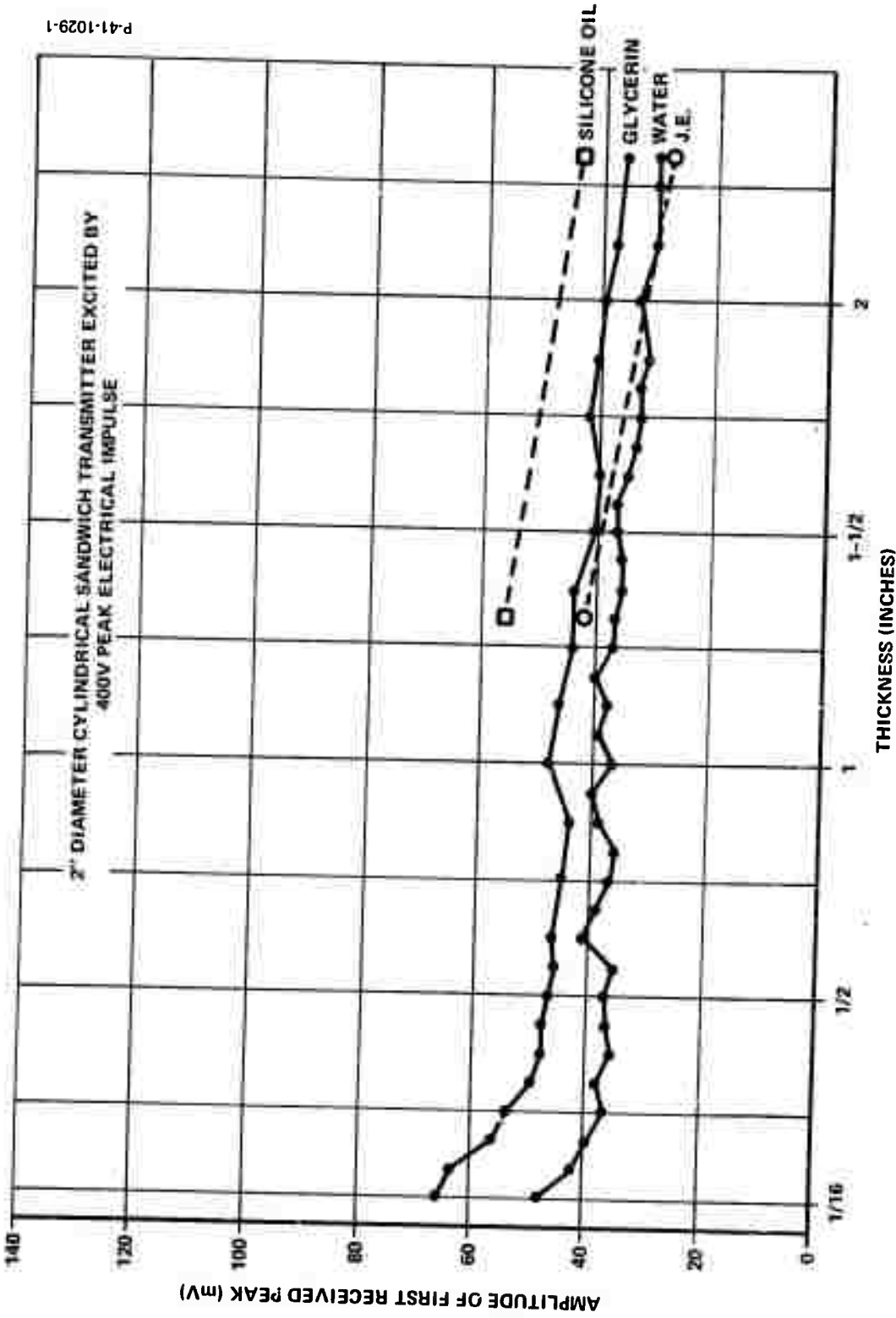
Figure 5-5 - Relative Transmission of Various Coupling Materials
Through 29-Inch Red Granite Having Rough Surface

5-7

using resonant transmitting and receiving transducers. In these tests, an (James Electronics) impulse generator was used to excite the resonant transmitter.

The experimental results indicate that under <u>transient response</u>:

(1) The transmission characteristics of a couplant are relatively independent of the thickness of the couplant, as would be expected from theoretical considerations.[5]

(2) Of various couplants evaluated, water, glycerine, and silicone oil provided satisfactory performance. However, the relative amplitude of the signal transmitted through these couplants was not the same as would be expected from theoretical considerations. For example, based on theory, the relative amplitude of the signal transmitted through water should be twice as large as that transmitted through silicone oil, and one and one-half times that transmitted through glycerine. The probable causes for this disagreement may be relatively more air bubbles trapped in the water and/or poorer wetting of water to the transducer and rock surfaces. Both of these problems are known to degrade coupling properties.

(3) Coupling efficiency is usually somewhat higher when energy is coupled to smooth rather than to rough surface rock.

These results indicate that in field applications where the rock surface is not excessively rough, contained fluid couplants, as shown in Figure 5-6, can be used. In applications where a rock surface is very rough and the contacting couplant fails to provide adequate acoustic contact, a noncontacting method of coupling might be used. This could be accomplished by maintaining a water jet (mixed with a wetting agent) between the transducer and the rock surface.
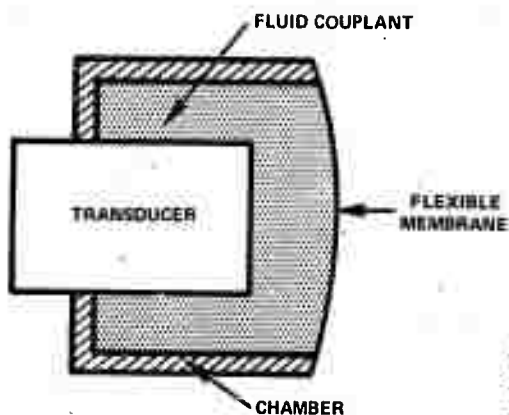
Figure 5-6 - Sketch of Transducer Coupling

5.5 REFLECTION TESTS

5.5.1 Instrumentation

The components of the pulse-reflection system used in the laboratory are shown schematically in Figure 5-3. Both resonant and nonresonant transducers were used. The resonant ones were the half-wavelength thick (Longevin-type) sandwiches which were later used in the field tests. In the laboratory reflection tests, for practical considerations such as simplicity and quickness, lubricating grease was usually used as a couplant.

The detected signals were usually first amplified by a amplifier (Hewlett-Packard 465A) and filtered by a bandpass filter. The amplified output was displayed on an indicator oscilloscope for an A-scan indication of travel times of the reflected signals.

5.5.2 Experimental Results

Unless otherwise stated, the reflection data presented below were obtained using a 5-inch diameter cylindrical sandwich transducer for the transmitter and a 2-inch diameter cylindrical sandwich transducer for the receiver. The lowest resonant frequency of the loaded transducer was 23 kHz.

REFLECTED SIGNAL

REFLECTED SIGNAL
FILTERED BY A BANDPASS
FILTER (50-200 kHz)

0.5V/DIV

TIME (0.2 MSEC/DIV)

EXPECTED ARRIVAL TIME
OF SIGNAL FROM
ROCK-AIR INTERFACE

a) Input source waveform is a (100V peak) single sinusoidal cycle at 23 kHz.

REFLECTED SIGNAL

REFLECTED SIGNAL
FILTERED BY A BANDPASS
FILTER (50-200 kHz)

0.2V/DIV

TIME (0.2 MSEC/DIV)

EXPECTED ARRIVAL TIME
OF SIGNAL FROM
ROCK-AIR INTERFACE
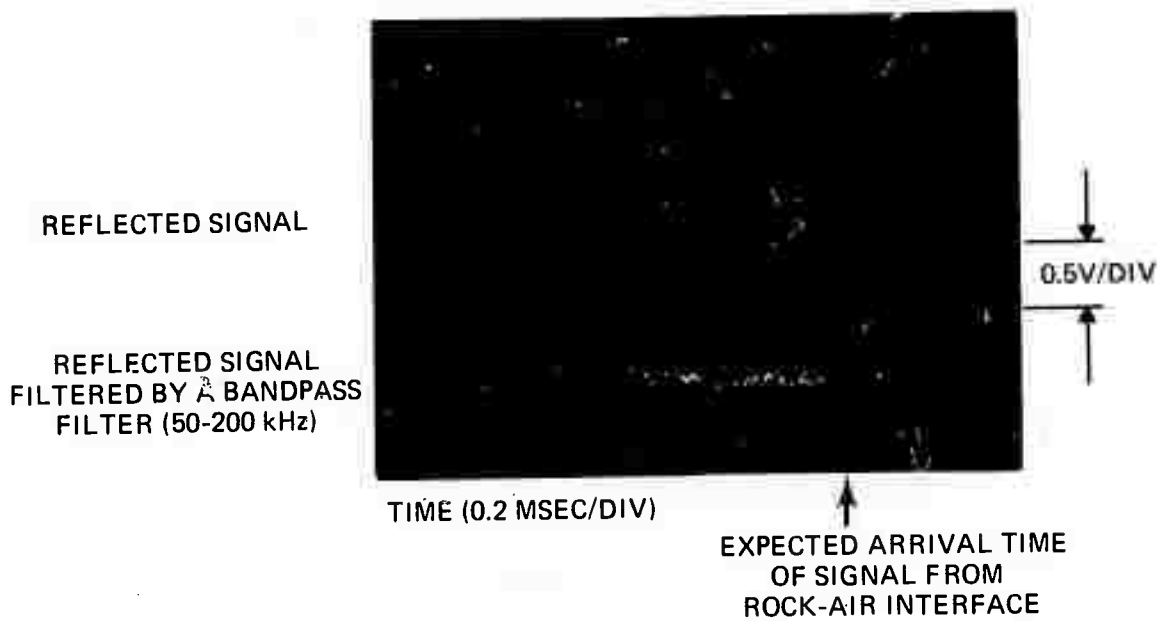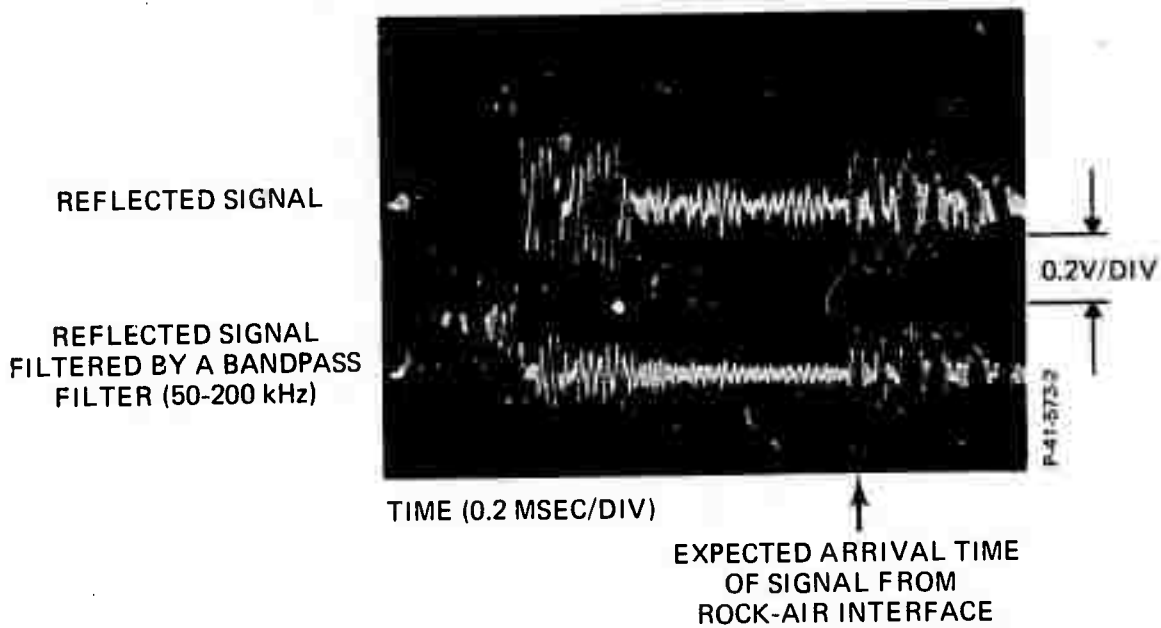
b) Input source waveform is a (100V peak) single sinusoidal cycle at 50 kHz.

Figure 5-7 – Reflected Signals From 12-Foot Thick Granite Block
(1' x 4' x 12')

REFLECTED SIGNAL

**REFLECTED SIGNAL
FILTERED BY A BANDPASS
FILTER (50-200 kHz)**

0.01V/DIV

TIME (0.2 MSEC/DIV

**EXPECTED ARRIVAL TIME
OF SIGNAL FROM
ROCK-AIR INTERFACE**

P-41-791-2
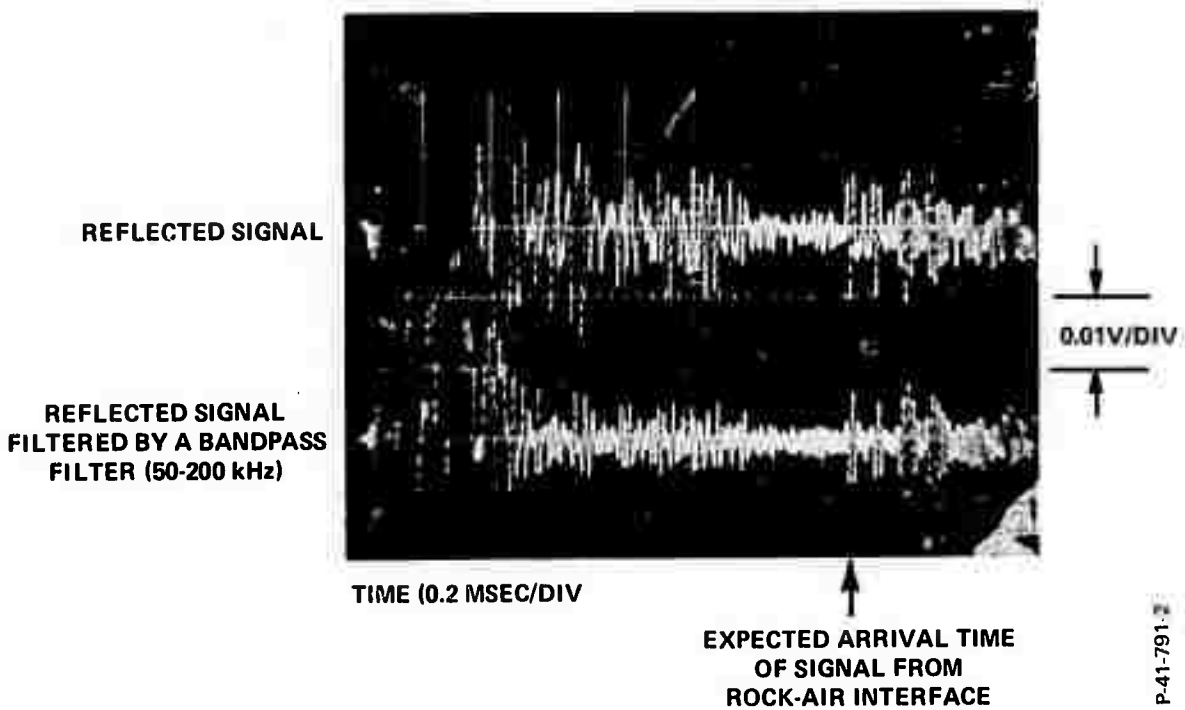
Figure 5-8 - Reflected Signals From 12-Foot Thick Granite Block
(1' x 4' x 12'). Input Waveform is a 100V 9-Microsecond
Wide Rectangular Pulse.

Figures 5-7 and 5-8 show results obtained on the rectangular granite block of size 1' x 4' x 12' with both transmitting and receiving transducers mounted in close proximity (less than 6 inches apart) on one of the corners of 1' x 4' surface. In all these figures, the top trace shows the signal detected by the receiver and the bottom trace shows the same detected signal which has been filtered by a bandpass filter passing signals from 50-200 kHz. In Figure 5-7(a), the transmitter excitation was a single sinusoidal cycle at 23 kHz; in Figure 5-7(b), a single sinusoidal cycle at 50 kHz. In Figure 5-8, the excitation was a 9-microsecond wide rectangular pulse. For the same input peak voltage, the reflected signal for the rectangular pulse excitation was an order of magnitude smaller than that for the single sinusoidal cycle excitation at 50 kHz. This is due to the fact that the rectangular pulse signal excited almost the total resonance spectrum of the transducer almost equally, whereas the single sinusoidal excitation cycle excited strongly only the closest resonant frequency (which resulted in improved performance for single sinusoidal cycle excitation at 50 kHz). In both filtered and unfiltered detected outputs, the signals reflected from the rock-air interface (located 12 feet from the transmitter-receiver interface) can be easily identified except in the unfiltered output obtained with the single cycle excitation at 23 kHz.

For the sinusoidal cycle excitation at 23 kHz, the dominant component in the detected signal in Figure 5-7(a) is at about 23 kHz which is the lowest resonant frequency of the transmitter; the next stronger signal component is at the resonant frequency of about 43 kHz. The pulse width of the acoustic signal generated in this case was about a millisecond long due to the high Q ($\sim$ 20) of the transmitter; therefore, the signals reflected from the desired rock-air interface (located at 12 feet away) were completely swamped by the surface waves reflected from the 90-degree corner of the granite block (which is 4 feet from the transmitter-receiver grouping). After the strong low-frequency (23 kHz) signals were filtered from the detected output, the 43 kHz signals reflected from the

air interface could be easily seen, as shown in the bottom trace of Figure 5-7(a).

In the reflection data presented, there are more than one reflected wavelets arriving at the transmitter-receiver interface from the rock-air interface located at 12 feet away due to multiple reflections within the granite block.

Reflections were also observed from the rock-air interfaces located 4' and 1' from the transmitter-receiver interface. Figure 5-9(a) shows the unfiltered and filtered reflected signals located 1 foot from the transmitter-receiver interface (transmitter and receiver were located in the center of the 4' x 12' surface of the granite block). The transmitter excitation is a single sinusoidal cycle at 50 kHz. In both unfiltered and filtered detected outputs, the reflected signals from the rock-air interface can be easily identified. Figure 5-9(b) also shows reflection data from the 1-foot deep rock-air interface when low-Q transmitting and receiving transducers were used. (Transmitter excited with 112 kHz single sinusoidal cycle.) Comparing Figures 5-9(a) and (b), it is seen that, although the high Q transducers are more efficient than the low Q ones, as expected, the resolution (signal-to-noise ratio) of the low Q transducers is better. For field work, both high transducer efficiency and good resolution are required. Since these are contrary requirements in terms of transducer Q, a compromise, using transducers with an intermediate Q value, may be necessary.

In another test, the low-Q transmitting and receiving transducers were located in close proximity over the smooth 29 x 37 inch rock-air interface of the block of size 8 x 29 x 37 inches (block A). Figure 5-10 shows the signal reflected from the rock-air interface which is located 8 inches from the transmitter-receiver interface. In this case, the transmitter is excited by a 0.05 milliseconds-wide, 50 to 200 kHz frequency-modulated (FM) pulse signal. The received signal shows an FM pulse (resembling the excitation pulse) reflected by the granite-air interface with good resolution. Similar results have been obtained with other types of excitation waveforms including narrow PM-CW signals.

REFLECTED SIGNAL

REFLECTED SIGNAL FILTERED BY A BANDPASS FILTER (50-200 kHz)

2V/DIV

1V/DIV

TIME (0.05 MSEC/DIV)

EXPECTED ARRIVAL TIME OF SIGNAL REFLECTED FROM ROCK-AIR INTERFACE

(a) INPUT WAVEFORM IS A 100V PEAK SINGLE SINUSOIDAL CYCLE AT 50 kHz

REFLECTED SIGNAL

REFLECTED SIGNAL FILTERED BY A BANDPASS FILTER (100-200 kHz)

0.02V/DIV

0.02V/DIV

P-41/2912

TIME (0.05 MSEC/DIV)

EXPECTED ARRIVAL TIME OF SIGNAL REFLECTED FROM ROCK-AIR INTERFACE

(b) INPUT WAVEFORM IS A 100V PEAK SINGLE SINUSOIDAL CYCLE AT 112 kHz (WITH LOW-Q TRANSDUCERS)

Figure 5-9 – Reflected Signals From a 1-Foot Thick Granite Block (1' x 4' x 12')

FREQUENCY MODULATED (FM) ELECTRICAL EXCITATION ACROSS THE TRANSMITTER

RECEIVED SIGNAL

200 V/DIV

.02 V/DIV

TIME (0.02 msec/div)

EXPECTED TIME OF ARRIVAL OF SIGNAL REFLECTED FROM ROCK-AIR INTERFACE
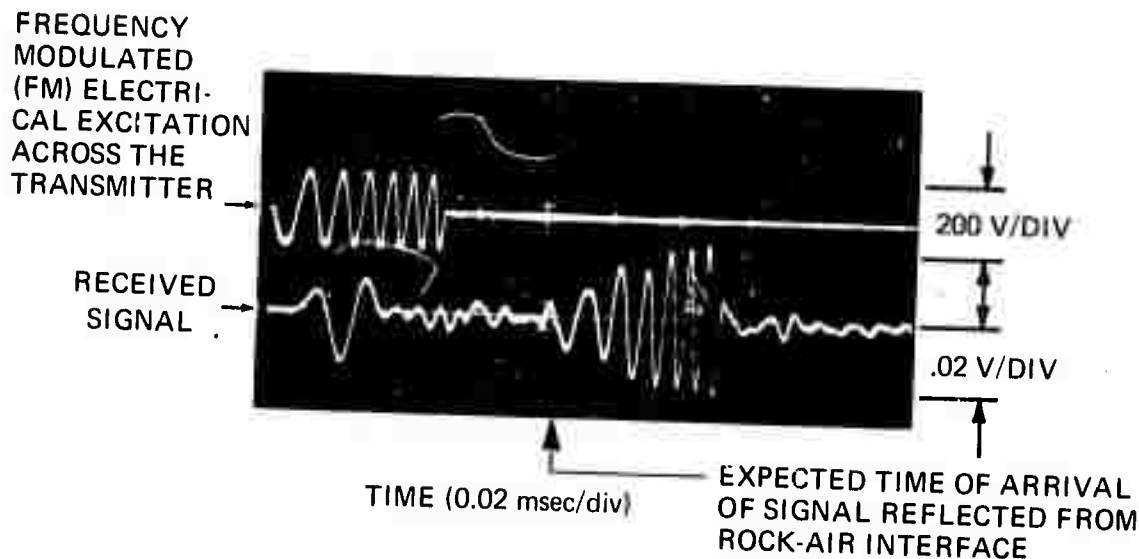
Figure 5-10 - Input Source Waveform is a (100V Peak) 50-200 kHz (0.05 msec wide) Frequency-Modulated Excitation Pulse

Figure 5-11 shows the signal reflected from the rock-air interface of block A which is located at 29 inches from the transmitter-receiver mounting surface. In this case, low-Q transducers were placed in close proximity over the rough (8 x 37 inches) surface of the rock. The transducers were coupled to the rough surface rock via lubricating grease. Some of the early arrivals at the receiver are direct surface waves and surface waves reflected from surface discontinuities. In addition, high-frequency signals are readily scattered back from the granular structure of the granite rock. These early arrivals can be removed from the received signal by cutting a slit between the transmitter and receiver locations. Figure 5-11(b) shows a received signal similar to the one shown in Figure 5-11(a) except that a 1/4-inch wide, 6-inch deep slit was cut between the transmitter and receiver, which were located in close proximity over the rough 8" x 29" rock-air interface. This method of cutting a slit for filtering surface waves is, however, not practical in most field applications.
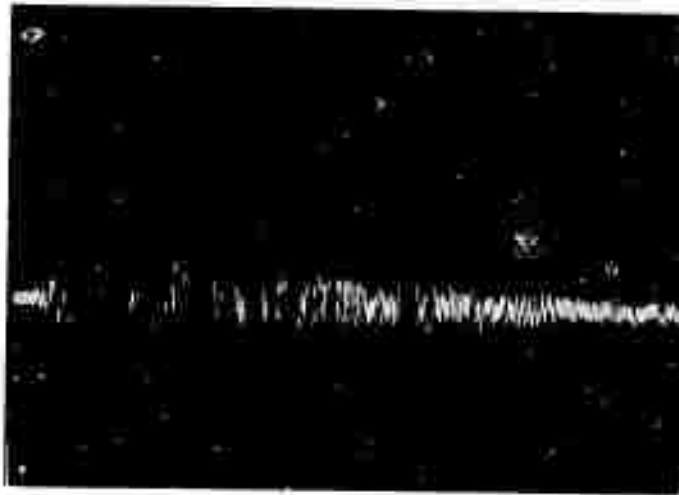
TIME (50 μSEC/DIV

(a) Reflected signal without a slit.
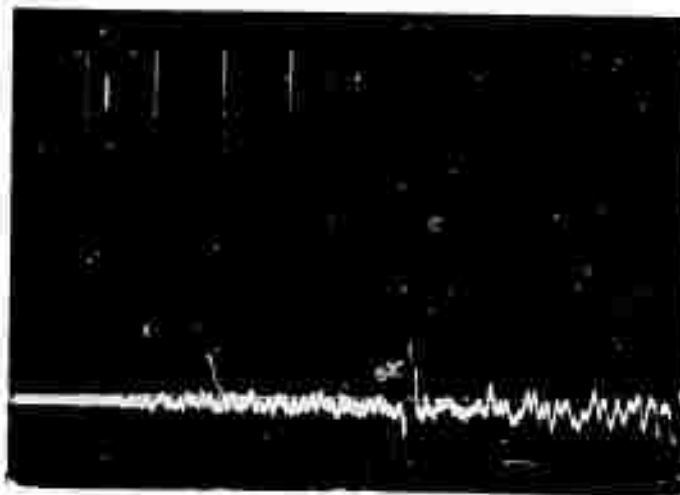
TIME (50 μSEC/DIV)

(b) Reflected signal with a slit.

Figure 5-11 - Effect of Cutting a Slit Between Transmitting and
Receiving Transducers

5.6 LABORATORY CONCLUSIONS

The laboratory results indicate that the pulse-reflection system used in the laboratory can detect reflections from the free surface of a homogeneous rock medium. Also, the acoustic energy can be equally well coupled into and out of rough (or smooth) surface rocks via glycerine, silicone oil, and water (mixed with a wetting agent).

Low-Q transducers are especially desired because they were found to distort very little the radiated or incoming acoustic waveform. The outgoing signal could therefore be made to resemble the excitation waveform very closely and thus provide a method of waveshaping the radiated acoustic signals. However, low-Q transducers are not as sensitive as high-Q transducers. A compromise should be made for a specific field test.

SECTION 6
FIELD EXPERIMENT

A field test was carried out in order to obtain acoustic reflection data from known structures of reasonable size so that the validity of the chosen approach could be determined. To minimize expenditure, existing equipment was used where possible with such modifications as were necessary.

6.1   SELECTION OF THE FIELD SITE

Because the geologic rock medium of interest is "hard" or crystalline rock, a field test site of this type was sought. The site should have known geological features which can be correlated with test results. The Edgar Mine (Colorado School of Mines Experimental Mine) located at Idaho Springs, Colorado, was selected for field experiments. It is a hard rock mine and has certain known geological features. The layout of the mine is shown in Figure 6-1. The tunnel walls have a destressed zone of crushed wallrock which ranges from a few inches to several feet in thickness; this zone was formed when explosives were used to excavate tunnels in this mine.

6.1.1   Selection of Test Sites Within the Edgar Mine

The selection of a test site inside the Edgar Mine was primarily guided by the following desired characteristics:

- The rock medium is hard or crystalline
- One of the surfaces of the test site is preferably the end-wall of a tunnel
- The site contains known geological features
- Both rock-air interfaces of the test site are accessible for measurements
- Overall thickness of the test site is a few tens-of-feet.
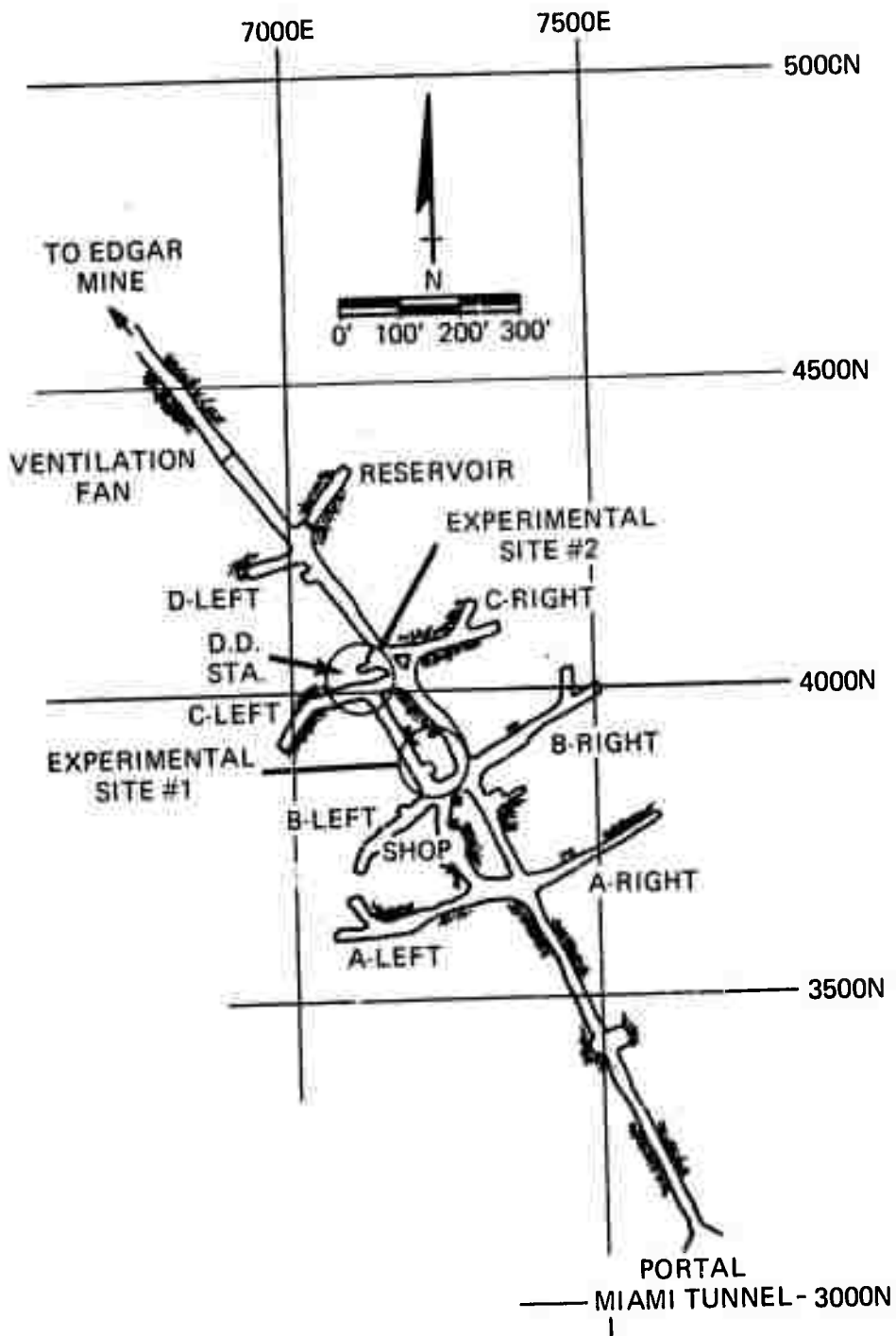
Figure 6-1 - Layout of the Experimental Mine of the Colorado
School of Mines

P-41-573-2

In the site selection process, we evaluated two different test sites inside the mine, as shown by the two circles in Figure 6-1. The sites are denoted by sites No. 1 and 2.

Site No. 1

This test site has the desirable features listed above; however the rock face forming the tunnel end-wall (on which transducers were mounted) was extensively jointed and weathered. There was also a large joint that ran diagonally across the tunnel end-wall. A photograph of the face of the tunnel end-wall is shown in Figure 6-2. The rock medium was about 30-feet thick between the opposite free surfaces of the rock. Continuous-wave acoustic signals could be transmitted through the rock medium at certain discrete frequencies within the frequency range of 2 to 10 kHz.

Transmission and reflection tests were conducted where the transmitter was excited by a narrow width high-voltage impulse (obtained from the James Electronics Impulse Generator). In these results, as shown in Figure 6-3, the dominant frequency in both transmitted and reflected signals is about 3 kHz, which was one of the discrete frequencies where strong transmission of continuous-wave acoustic signals was earlier observed. The discrete-frequency behavior does not seem to be related to either transmitting or receiving circuits because the transmitted and received signals using flat-response receivers showed similar behavior when hammers of different weights and shapes were used to generate acoustic signals. Figure 6-4, for example, shows the transmitted and reflected signals when a claw hammer impacted the rock as an acoustic source. In view of these results, it appears that this discrete-frequency phenomenon is related to some physical parameter (or parameters) of the rock medium under investigation. A plausible candidate parameter could be the destressed zone where a resonance is set up within the thickness of the destressed zone of the tunnel walls. The thickness of this zone is known to vary anywhere from a few inches to a few feet. In order to better understand and possibly isolate the

Figure 6-2 - Rock-Air Interface at Site No. 1

REFLECTED
SIGNAL

TRANSMITTED
SIGNAL

TIME (1 MSEC/DIV)
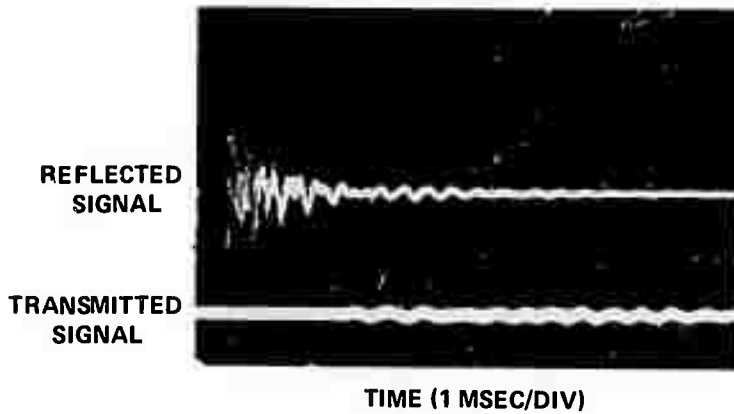
(a) REFLECTED AND TRANSMITTED SIGNALS DUE TO EXCITATION
AT ROCK-AIR INTERFACE SHOWN IN FIGURE 6-2

TRANSMITTED
SIGNAL
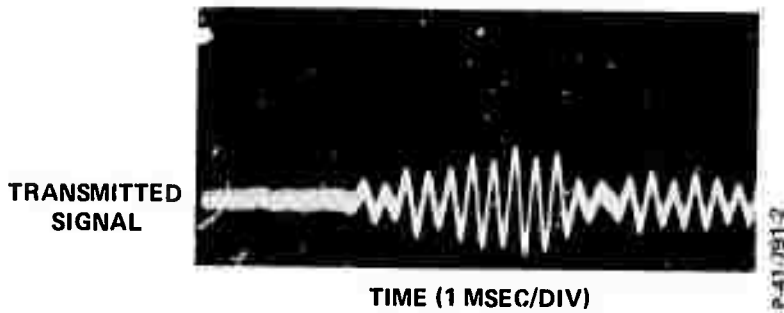
TIME (1 MSEC/DIV)

(b) TRANSMITTED SIGNAL (EXCITATION AT OPPOSITE SIDE OF
THAT IN FIGURE 6-3a)

Figure 6-3 - Impulse Excitation at Site No. 1

TRANSMITTED
SIGNAL
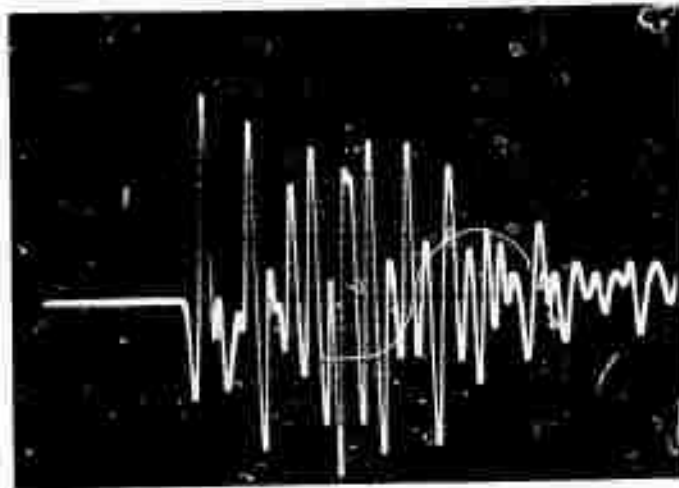
REFLECTED
SIGNAL
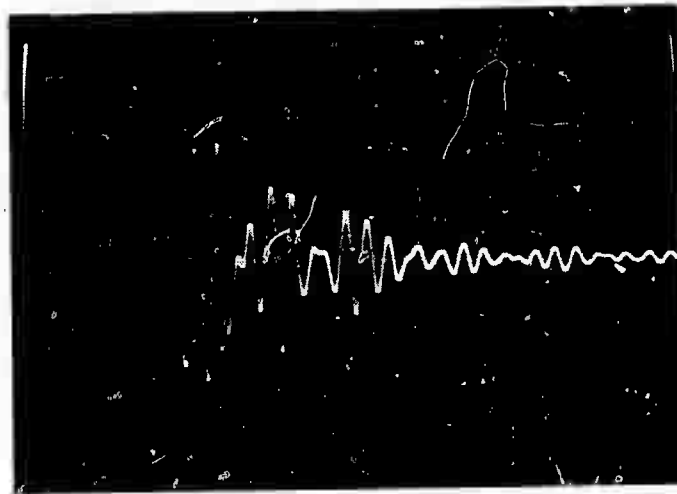
TIME (1 MSEC/DIV)

P-41-791-2

Figure 6-4 – Transmitted and Reflected Signals Due to Claw-Hammer
Impact at the Rock Face (Shown in Figure 6-2) at Site No. 1

rock parameters responsible for the discrete-frequency behavior, we decided to move to another site, called Site No. 2.

Site No. 2

Site No. 2 has all the desirable features of a potential test site. It had fewer joints, and the rock medium was relatively homogeneous except for two fracture zones visible from outside.

At this site, the experiments conducted at test site No. 1 were repeated. The results at Site No. 2 showed a similar discrete-low-frequency behavior of the rock medium. A refraction test was conducted (shown in Figure 6-5) which indicated that there is a low-velocity rock medium about a couple of feet in thickness which overlies a high-velocity rock medium. The longitudinal wave velocities in the low and high velocity media were found to be 14,900 and 17,900 ft/sec., respectively. The results of a resonance test using drill noise as the sound source (to be discussed later) indicated the presence of a discontinuity at a depth varying from 1 to 5 feet below the rock face. In view of the refraction and resonance test results, the discrete-low-frequency behavior of the

DETECTED OUTPUT
AT 44' AWAY FROM
THE HAMMER IMPACT

TIME (1 MSEC/DIV)
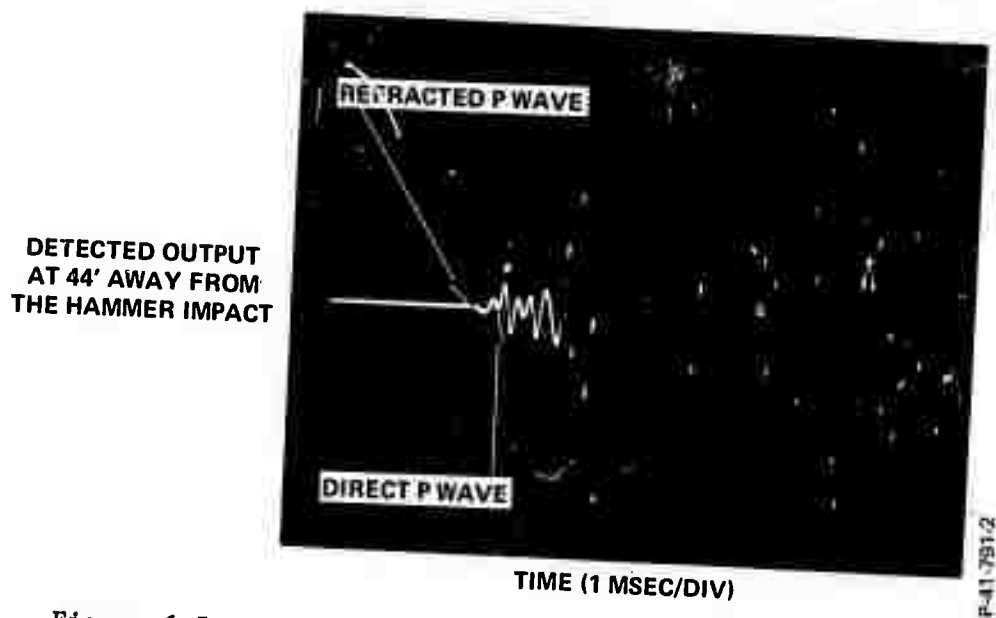
Figure 6-5 – Refraction Test Conducted at the Rock Face C-Left (Shown in Figure 6-6) at Test Site No. 2

rock can be explained by the setup of thickness resonances in the destressed zone of the tunnel walls of the mine.

The presence of the discrete-low-frequency behavior of the rock will not alter the direction of the research program outlined earlier since such low-frequency signals can be filtered out from the detected signals.

Site No. 2 was selected to carry out extensive field experiments since this site, as compared to Site No. 1, had fewer joints and the rock medium was relatively homogeneous.

6.1.2   Detail of Field Test Site No. 2

This site is shown in detail in the floor plan given in Figure 6-6. Pulse-reflection tests were conducted from rock face locations at both C-left and DD Stn. On the three sides of this site, there was a 7- to 8-foot high tunnel. The tunnel at DD Stn ended about 12 feet from the transducer mounting location. The photographs of the rock faces at C-left and DD Stn are shown in Figure 6-7. A photograph of the main track joining tunnel "C-left" and tunnel "DD Stn" is shown in Figure 6-8, where tunnel C-left is on the left side and tunnel DD Stn is on the right side. The rock at C-left is weathered and stained medium-grained biotite gneiss, whereas the rock at DD Stn is medium-grained quartz diorite gneiss. (The holes that are seen in these photographs were drilled by students of the Colorado School of Mines and have no connection with this work). In the main track between C-left and DD Stn, there were two clearly observable zones of fractured rock material. From the strike and dip measurements, an effort was made to determine if the fracture zones emerged at other points in the tunnel; however, no such outcropping was observed.

The surface rock sizes varied from 1 foot to 4 feet. The rock face was extremely jointed; however, areas could be found in which the rock face was solidly connected to more competent rocks. Transmitting and receiving transducers were located on the competent rock at both sides of the test site. The path length between transducers at
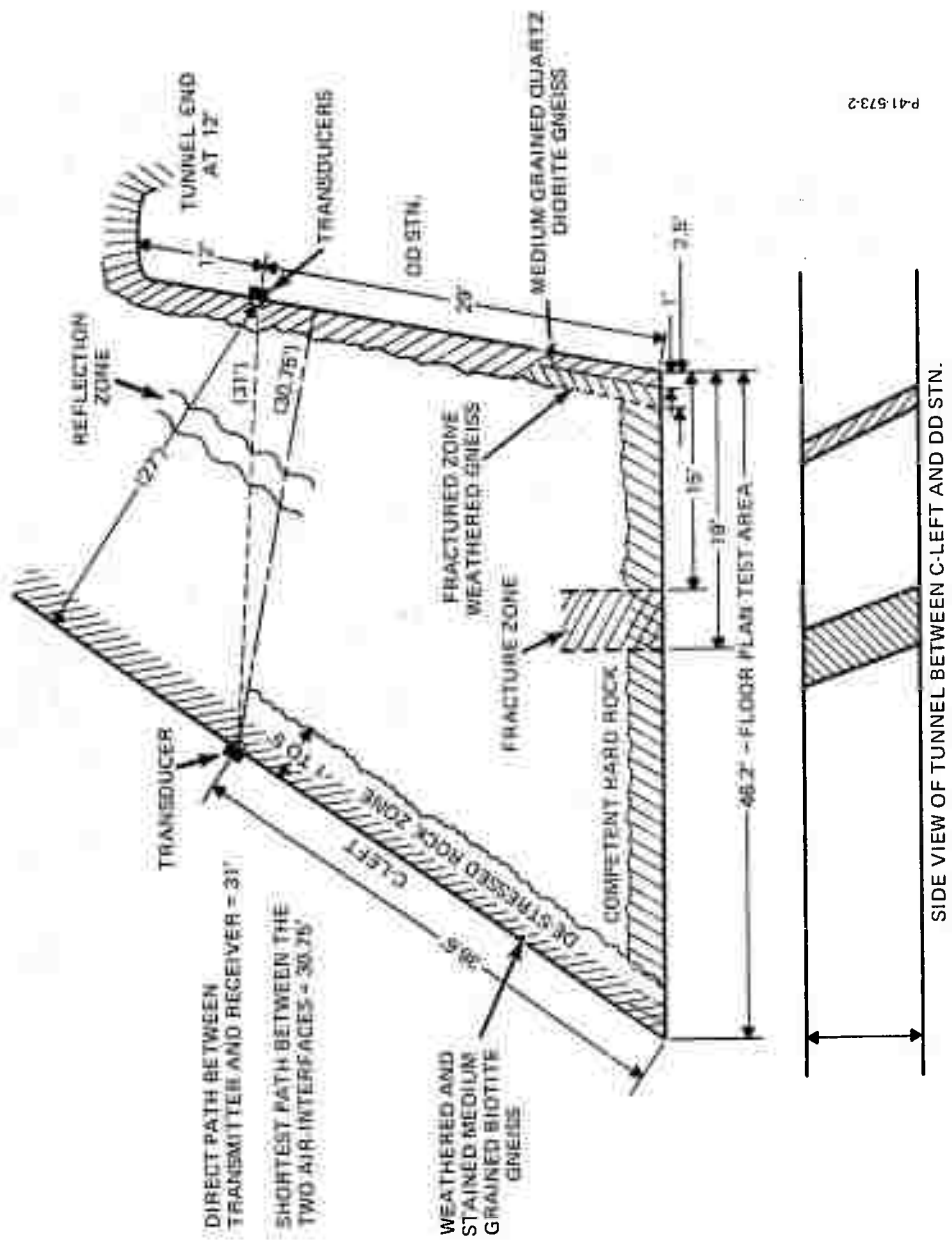
Figure 6-6 - Detail of Experimental Site

(a) ROCK FACE AT C-LEFT

(b) ROCK FACE AT DD STN.

P-41-791-2

Figure 6-7 - Photographs of the Rock Faces at Site No. 2

Figure 6-8 – Photograph of the Tunnel Between C-Left
and DD Stn at Site No. 2

C-left and DD Stn was about 31 feet. The shortest acoustic path length between the C-left transducer and the DD Stn air-interface was about 30.75 feet; between the DD Stn transducer and the C-left air-interface, about 27 feet.

6.2 PULSE-REFLECTION TESTS

At both C-left and DD Stn, several pulse-reflection experiments were carried out. For ease of mounting, the transducers were cemented to the rock face using dental impression plaster;[12] however, in future field situations, fluid couplants (recommended earlier) will be used. The components of the pulse-reflection detection system used in the field tests are shown schematically in Figure 6-9. Due to the jointing of the rock face at the field site, three receivers could not be advantageously located over a solid rock race as needed for delineating a sloping planar interface. Therefore, at this field test site, reflection data were obtained using a single receiver.

Three classes of electrical excitation waveshapes appropriate for exciting a transmitter were used. A broad range of electrical excitation frequencies was used to determine the optimum operating frequency range for this field application. These were

- Single sinusoidal cycle (f = 220, 100, 27.5, 23, 17.5 kHz).
- Pulse-modulated continuous wave (PM-CW) signals (f = 27.5, 23, 17.5, 7.75 kHz).
- Frequency modulated (FM) pulse signals (f = 6 to 18, and 18 to 30 kHz).

The pulse repetition frequency of the excitation signals was 20 Hz. All of the field data were recorded on magnetic tapes.

The high-frequency single sinusoidal cycle transmitter excitations at 220 and 100 kHz were chosen to excite higher transducer resonances and thus obtain radiated acoustic signals of relatively narrow pulse width. With these narrower pulses, shallower discontinuities, which otherwise may not be detectable with signals of long pulse width and low frequency, can be detected with reasonably good resolution.
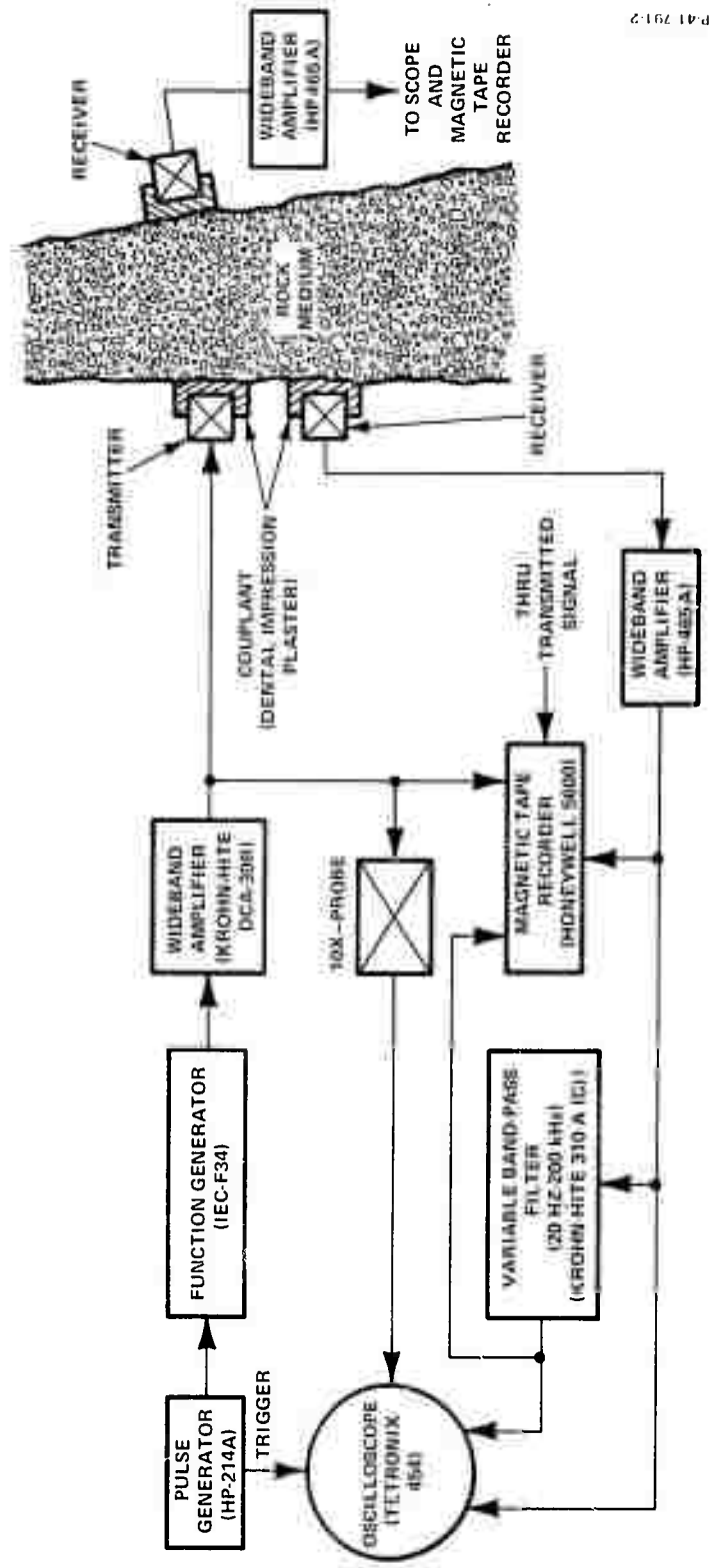
Figure 6-9 — Pulse-Reflection System Instrumentation in the Field Test

In addition to their use in detecting shallower discontinuities, narrow pulse-width, high-frequency signals can provide a means of seeing deeper discontinuities if time-averaging signal enhancement techniques are applied to the detected signal. The time-averaging method will be discussed in the next section.

In addition to these higher excitation frequencies, lower excitation frequencies of 17.5, 23, and 27.5 kHz were chosen to provide lower-frequency radiated acoustic pulses which hopefully would provide reasonable signal-to-noise ratios, although these ratios may be attained at the expense of relatively broad pulses. The excitation frequency of 23 kHz (which is also the lowest and dominant resonant frequency of the transmitter) was specifically chosen because it radiated the strongest pulse into the rock. The excitation frequencies of 17.5 and 27.5 kHz were chosen so as to excite the transducer a little off-resonance in order to radiate relatively narrower pulses than the one at 23 kHz. Finally, the excitation frequency of 7.75 kHz was experimentally selected because it gave the highest amplitude of the return signals.

Some of the field data from these experiments are shown in Figures 6-10 and 6-11. The signals recorded at both the test sites (i.e., C-left and DD Stn) were detected by a resonant receiver located in close proximity to the transmitter. Except in Figure 6-11(b), all recorded signals have been filtered by a bandpass filter (6-30 kHz).

Figures 6-10(a) and 6-10(b), respectively, show the reflected signals due to a 17.5 kHz single sinusoidal cycle and an 0.4-millisecond (6-18 kHz) FM excitation of the transmitter at C-left. The signal reflected from the air-interface at DD Stn is expected to arrive after a round-trip delay time of 4.05 milliseconds (which corresponds to a round-trip travel distance of 61.5 feet), as shown by the arrow.

Figures 6-11(a) and 6-11(b) show the reflected signals due to 0.4 millisecond-wide, PM-CW signals at 17.5 kHz and 7.75 kHz, respectively. The signal reflected from the air-interface at C-left is expected to arrive after a round-trip time delay of 3.6 milliseconds (which corresponds to a round-trip travel distance of about 54 feet), as shown by the arrow.

REFLECTED SIGNAL
FILTERED BY A
BANDPASS FILTER
(6-30 kHz)
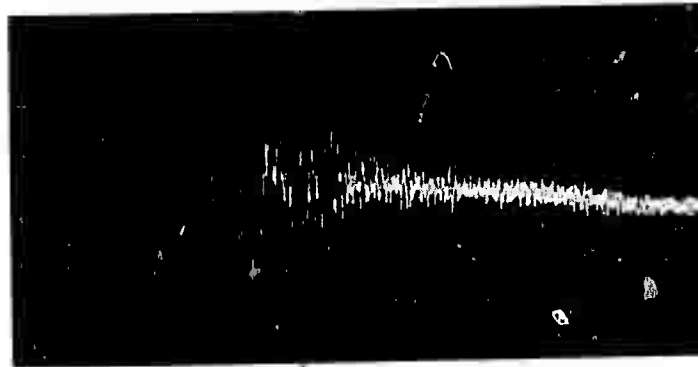
TIME (1 MSEC/DIV)

(a) REFLECTED SIGNAL DUE TO A SINGLE SINUSOIDAL
CYCLE AT 17.5 kHz

REFLECTED SIGNAL
FILTERED BY A
BANDPASS FILTER
(6-30 kHz)
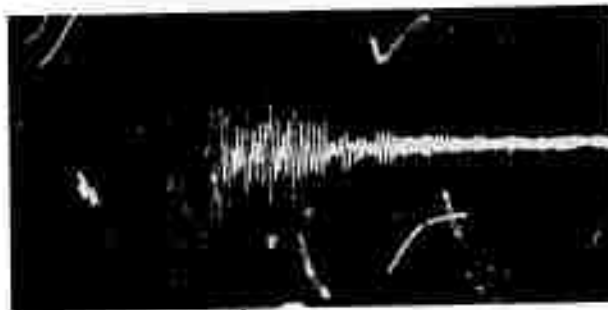
TIME (1 MSEC/DIV)

EXPECTED ARRIVAL TIME OF
REFLECTED SIGNAL FROM
ROCK-AIR INTERFACE
(AT DD STA.)

(b) REFLECTED SIGNAL DUE TO 0.4 MSEC WIDE
6-18 kHz FM PULSE SIGNAL (AT C-LEFT)

P-41-791-2

Figure 6-10 - Reflection Field Data at C-Left

REFLECTED SIGNAL
FILTERED BY A
BANDPASS FILTER
(6-30 kHz)
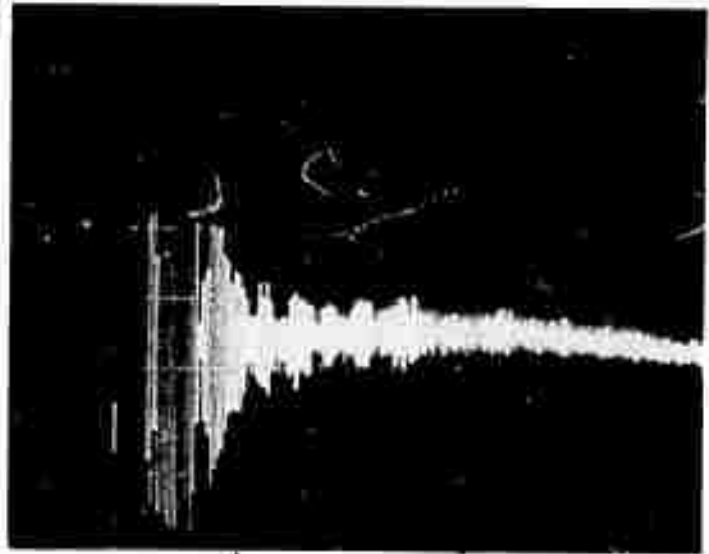
TIME (1 MSEC/DIV)

(a) REFLECTED SIGNAL DUE TO AN 0.4 MSEC WIDE
17.5 kHz PM-CW SIGNAL AT (DD STA.)

REFLECTED SIGNAL
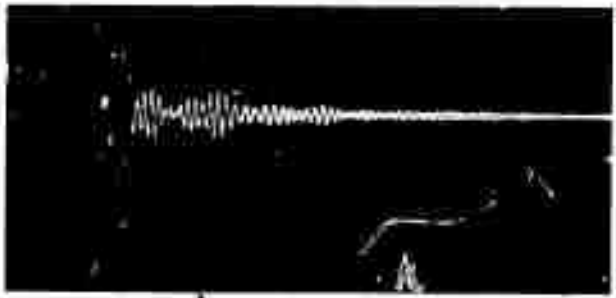
TIME (1 MSEC/DIV)

EXPECTED ARRIVAL TIME
OF REFLECTED SIGNAL FROM
C-LEFT ROCK-AIR INTERFACE

(b) REFLECTED SIGNAL DUE TO AN 0.4 MSEC WIDE
7.75 kHz PM-CW SIGNAL (DD STA.)

P-41-791-2

Figure 6-11 - Reflection Field Data at DD Stn

At the expected arrival time, a relatively large signal can be clearly seen, especially in the case of the low-frequency PM-CW excitation signal.

Figures 6-12(a) and 6-12(b) show the reflected signal, respectively, due to a 220 and 100 kHz single sinusoidal cycle excitation of the transmitter located at C-left. In these figures, there is a large signal wave packet arriving at a time delay of about 0.6 milliseconds, as shown by the arrow; this time delay corresponds to a round-trip travel distance of about 8-10 feet. This could be the reflection from the discontinuity layer (destressed zone) at a depth of about 4 feet.

6.3 RESONANCE TEST

A field experiment was undertaken to determine if excavation machine noise could be advantageously used as a sound source in a resonance method for detecting the thickness of the first discontinuity layer beyond the excavation face. At the C-left rock face a pneumatic drill was used to drill a hole to the depth of about 3 feet. Three receivers located on this surface were used as receivers. Signals were recorded for about one minute during the drilling operation, and then analyzed in the frequency domain on a real-time spectrum analyzer. (The spectrum analyzer is a model UA-6 and is manufactured by Federal Scientific Corporation).

The frequency spectrum analyses of the drill noise (as shown in Figure 6-13) show predominant signals at frequencies ranging from 3 to 7 kHz. This observed frequency range spectrum indicates the presence of a discontinuity layer below the rock face at a depth of about 1 foot to 2.5 feet. These results are consistent with the refraction data as well as the reflected signals shown in Figure 6-12. The results of this test suggest that drill noise could be used as a potential acoustic source for resonance detection; however, it is limited to cases where the discontinuity interface is parallel to the excavation face.

6.4 DATA PROCESSING PROCEDURES

In the laboratory investigations, signals reflected from known discontinuities can be easily identified in the detected signals. However,

REFLECTED FILTERED* SIGNAL
DUE TO A SINGLE
CYCLE EXCITATION
220 kHz
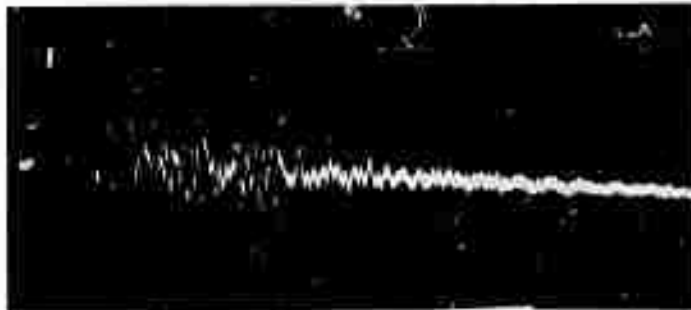
*BANDPASS
FILTER
SET AT
6-30 kHz

REFLECTED FILTERED* SIGNAL
DUE TO A SINGLE
CYCLE EXCITATION
AT 100 kHZ
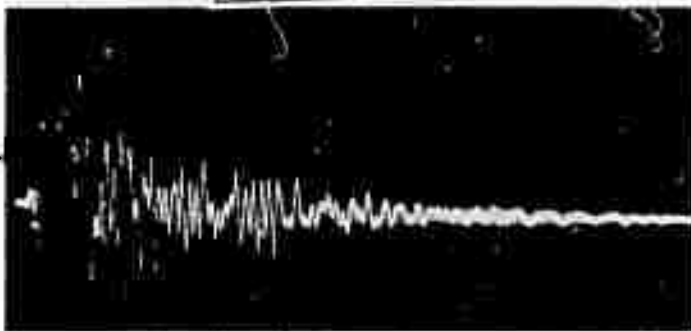
TIME (0.2 MSEC/DIV)

REFLECTION TIME CORRESPONDING
TO A DISCONTINUITY DEPTH
OF ABOUT 4 FEET

P-41-791-2

Figure 6-12 - Reflection Data at C-Left Due to High-Frequency
Single Cycle Excitations of the Transmitter at C-Left

RECEIVER NO. 1

RECEIVER NO. 2

RECEIVER NO. 3

0
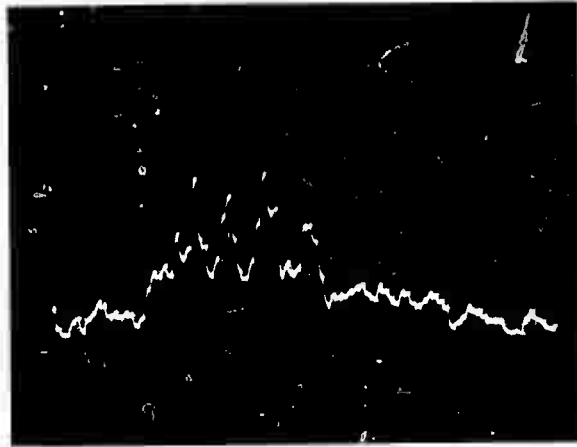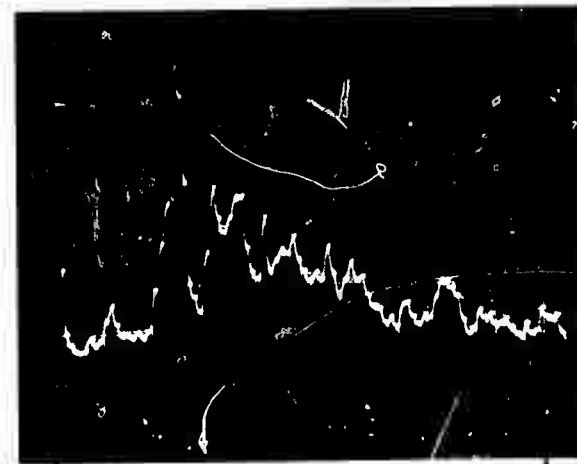
13.12 kHz

FREQUENCY (1.32 kHz/DIV)

P-41-791-2

Figure 6-13 - Frequency Spectra of Drill Noise Generated by
a Pneumatic Drill

such was not the case in the field data, because the rock medium at the test site was nonuniform and had geological characteristics far more complex than those of the homogeneous rock used in the laboratory test.

In order to identify the reflected signals from geologic discontinuities and the free surface of the test site, signal processing is required to enhance the desired signal in the presence of interfering noise and undesired coherent signals (for example, surface waves). Two signal enhancement techniques applicable to these field data are cross-correlation and time-averaging.

Cross-correlation is a method of time-domain analysis. This method establishes the similarity between two signal waveforms as a function of their mutual delay and is expressed by the degree of correlation and relative timing of the waveforms. A peak in the correlator output is observed when two time-shifted waveforms are alike in wave shape. The relative height of this peak increases directly with the degree of alikeness; its sharpness increases as the bandwidth of the correlation function increases. This technique is therefore a powerful analytical tool capable of providing discrimination against interference on the basis of waveform differences.

A time-averaging method of signal enhancement is useful where the (desired) repetitive signals are buried in random noise; the actual wave shape of the repetitive component can be extracted by the time-averaging technique, even if these signals are many times smaller than the noise. The principle of signal recovery is to extract a coherent pattern by repeatedly examining a desired portion of the waveform following a synchronizing pulse. The coherent pattern is reinforced at each repetition but any noncoherent noise present in the signal averages to zero.

6.4.1 Cross-Correlation

Cross-correlation permits the comparison of two time-varying functions $f_1(t)$ and $f_2(t)$. The resulting correlation function contains information regarding the frequencies that are common to both

waveforms, and the phase difference between them. Formally, the cross-correlation function is defined by[13]

$$C_{12}(\tau) = \text{L}_{\text{im}_{T \to \infty}} \frac{1}{2T} \int_{-T}^{T} f_1(t) \, f_2(t+\tau) \, dt \qquad (6\text{-}1)$$

where

$\qquad C_{12}(\tau)$ = the cross-correlation function

$\qquad\qquad T$ = the actual period of time over which the integral
$\qquad\qquad\qquad$ is computed

$\qquad\qquad \tau$ = the time-delay parameter

$f_1(t)$ and $f_2(t)$ are the two time-varying functions that arise from the physical process being investigated.

In our problem, the received signal is a superposition of (a) the desired reflected signals, (b) the undesired (usually strong) coherent signals, and (c) incoherent signals. In order to locate and identify the desired reflected signals, we need a function $f_2(t)$ which closely resembles the expected reflected signal. A waveform that is readily available for correlating the detected signal is the input wave-form, i.e., the excitation signal. The signal reflected from a discontinuity is expected to contain the input waveform although highly modified by the characteristics of the transmitter, receiver, coupling medium, and rock medium. The input signals modified by the system characteristics appear to be a good choice for the function $f_2(t)$, especially in cases where PM-CW or FM pulse excitations are used. The case of FM excitation is expected to provide a sharper correlation function than the one that uses the same pulse-width PM-CW signal because of the wider bandwidth of the FM signal.

Another possible approach for locating the presence of reflected signals is to examine the detected signal for changes in phase which generally occur wherever a new signal wave packet arrives at the detector. This could be accomplished by cross-correlating the detected

signal with a phase-detection waveform.[14] This non-conventional correlation approach differs from the previously discussed approach in which the similarity in wave shape was searched. An example of the effectiveness of cross-correlating a simple sinusoidal function $f_1(t)$ with a phase-detection waveform $f_2(t)$ is shown in Figure 6-14. Appendix B presents the mathematical derivation of the correlation function for a simple case of a sinusoidal function.

Both input excitation waveforms and appropriate phase-detection waveforms have been used to analyze the field data. The results are presented in Section 6.5.

6.4.2 Time-Averaging

A possible disadvantage to the use of cross-correlation for signal enhancement is the need to know the waveform of the desired reflected signal. The time-averaging technique does not require any knowledge of the desired reflected signal. It can be used effectively to enhance repetitive signals in random noise.

The signal-to-noise voltage ratio is improved in proportion to $\sqrt{N}$ where N is the number of repetitions. However, if the interference is from coherent signals, time-averaging does not provide improved signal-to-noise ratio because there is a buildup of both desired and undesired coherent signals, and the desired reflections cannot be distinguished from coherent noise.

6.5 FIELD DATA PROCESSING

Two sets of field data were processed. The first set is comprised of those field experiments where the transmitter was excited by a single sinusoidal cycle at a frequency of either 220 or 100 kHz. The second set included all other reflection experiments.

The time-averaging method of signal enhancement was used to process the first set of experiments. In these data, the desired reflected signals from the rock-air interface were observed to be buried in the random system noise.

The cross-correlation method of signal processing was used for the second set of data. In these data, at the expected times of arrival of
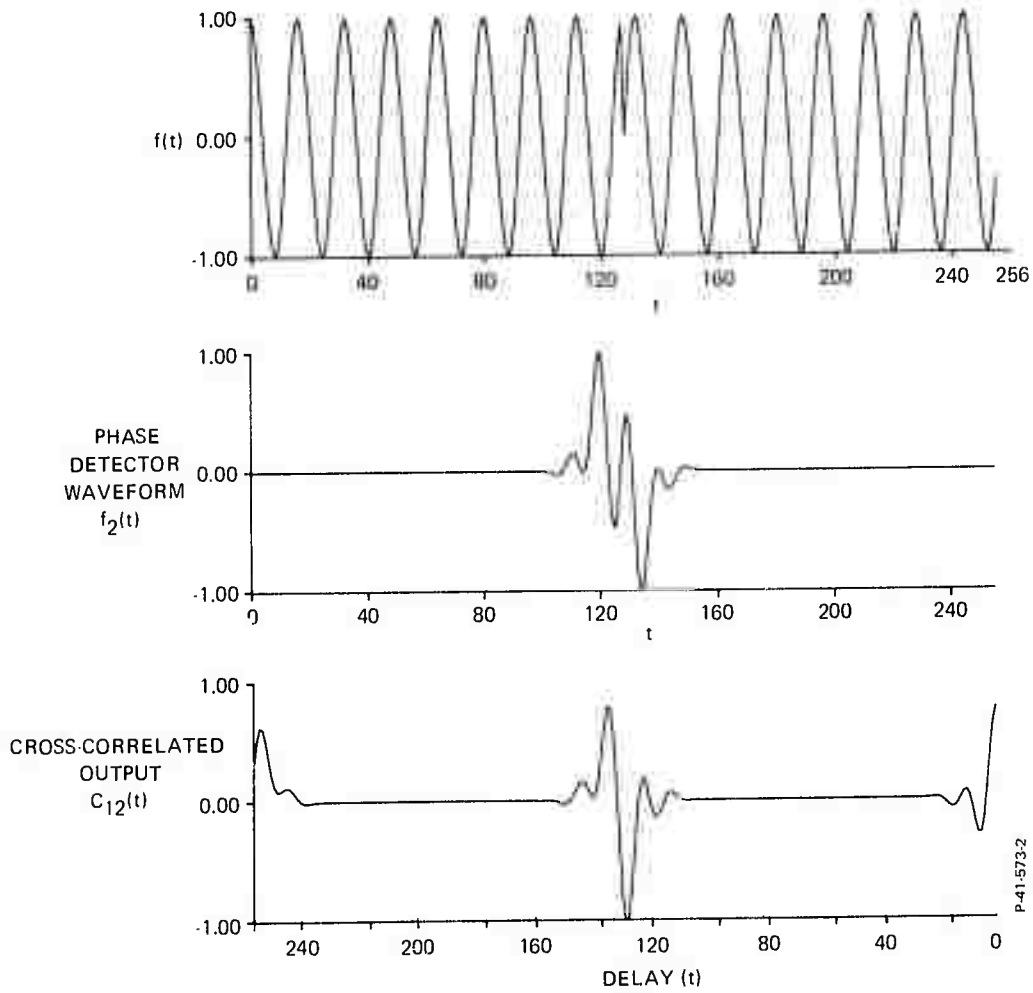
Figure 6-14 - Correlation Using Phase Detection Waveforms

desired reflected signals, coherent signals intermixed with other (undesired) coherent signals were observed, and consequently the desired reflected signals could not be identified.

A portion of the recorded field data were digitized for the cross-correlation method of signal enhancement; analog field data were however used for the time-averaging method of signal enhancement.

6.5.1 Time-Averaging of Field Data

In the field experiment, the transmitter at C-left was excited by a single sinusoidal cycle at a frequency of 220 kHz. Time-averaging was performed using the signal recovery mode of the Hewlett-Packard correlator (model 3721A).

The time-averaging of the detected signal, shown in Figure 6-15(b), at the expected time of arrival, shows an appearance of a single cycle of coherent signal at a frequency of about 45 kHz. Although the transmitter was excited at 220 kHz sinusoidal pulse, the frequency spectrum of the reflected signal (shown in Figure 6-15(a)) shows that the largest energy is radiated by the transmitter at about 45 kHz. However, the frequency spectrum analysis of the thru-transmitted signal does not show any sign of transmitted signals at about 45 kHz. In view of the inconsistency in the reflected and transmitted signal frequency spectra, it is difficult to be confident that the coherent waveform observed at the expected time of arrival is the reflected signal from the free surface.

6.5.2 Cross-Correlation of Field Data

A computer program was written to cross-correlate the detected output with either the source excitation waveform or the phase-detection waveform. Fast Fourier-transform techniques, based on the Cooley-Tukey algorithm (known as FFT), have been used to digitally cross-correlate two sampled time-varying functions $f_1(t)$ and $f_2(t)$.

In the earlier discussions of the cross-correlation of the detected output data with the excitation waveform, it was suggested that
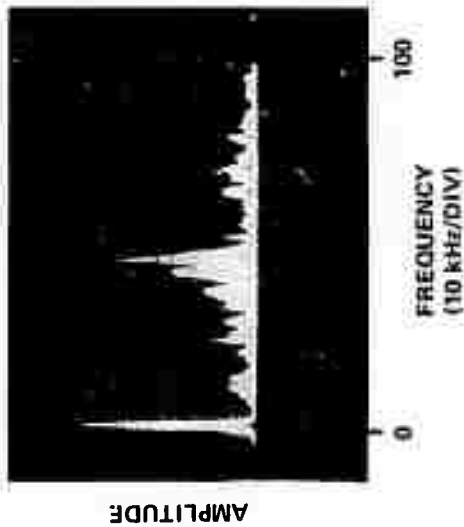
(a) FREQUENCY SPECTRUM
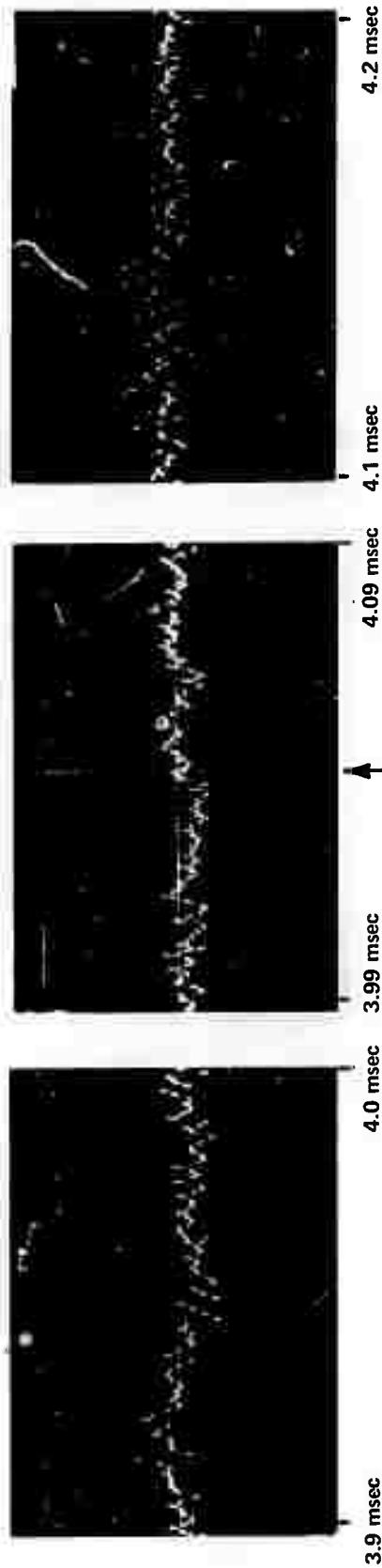
(b) TIME AVERAGING OF REFLECTED SIGNAL

Figure 6-15 – Time Averaging of Reflected Signal (Input Source Waveform is a Single 220 kHz Sinusoidal Cycle Pulse)

the excitation waveform be modified to compensate for the effects of such system parameters as the coupling medium and frequency-dependent attenuation in the rock medium. In the cross-correlation processing of field data, however, we have used the unmodified excitation waveform because of lack of specific data required for modifying the excitation waveform at this time. Correlation has been applied with a measure of success to the data obtained from experiments at C-left and DD Stn.

Figure 6-16(a) shows an example of the correlated functions for the cases where the transmitter at C-left is excited by (1) 17.5 kHz PM-CW and (2) 6-18 kHz FM pulse. The detected signals are correlated with the excitation pulse in both cases. The correlation peaks, shown in Figure 6-16(a), and other similar experiments have been plotted as a function of round-trip travel time in Figure 6-16(b). This figure shows that the destressed zones at C-left and DD Stn as well as the rock-air interface at C-left can be detected. In addition, a correlation zone at a round-trip travel time of about 2.8 msec was observed, which cannot be correlated with any known reflecting layer or zone. Tentatively, the cause of this correlation zone has been identified as a reflection zone in the interior.

An example of correlation results for the case where the transmitter at DD Stn is excited by a PM-CW signal at 7.75 kHz is presented in Figure 6-17(a). The upper trace is obtained when the detected signal is correlated with the excitation pulse, whereas the lower trace is obtained with a phase-detection waveform, as described in Section 6.4.1. The correlation peaks of the correlation functions shown in Figure 6-17(a) and other similar experiments have been plotted in Figure 6-17(b) as a function of round-trip travel time. Again in Figure 6-17(b), the destressed zone at DD Stn and the air-interface at C-left are observable. Additionally, a correlation zone at the round-trip travel time of about 1.4 msec was observed, which cannot be correlated with any known

CROSS-CORRELATION
OUTPUT FOR THE
400 μSEC PM PULSE
(17.5 kHz)
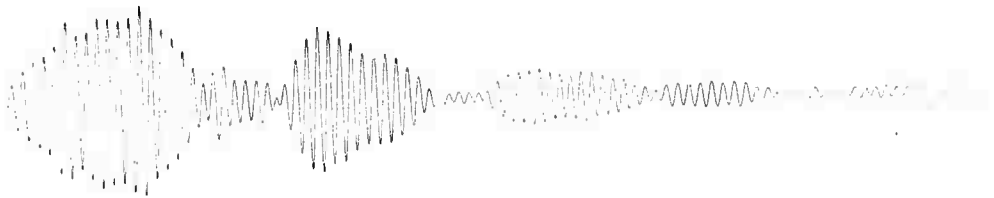
CROSS-CORRELATION
OUTPUT FOR THE
400 μSEC FM PULSE
(6-18 kHz)

0   0.975   1.95   2.925   3.9   4.875
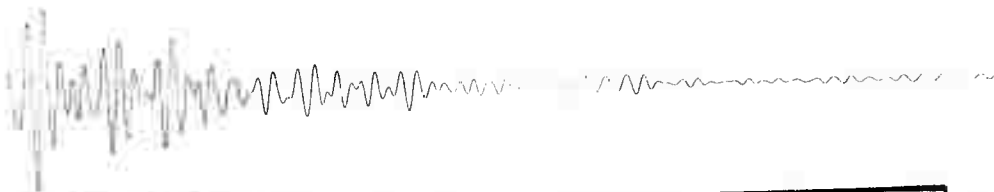
ROUND TRIP TRAVEL TIME FROM TRANSMITTER AT C-LEFT

(a) Correlation Results

S-SURFACE WAVES

P-P REF. FROM DESTRESSED-ZONE

SHEAR REF. FROM ROOF

P-P REF. FROM REFLECTION ZONE IN THE INTERIOR

P-P REF. FROM DESTRESSED ZONE DD STN.

P-P REF FROM AIR-INTERFACE DD STN.

EXCITATION   CORRELATION FUNCTION

PM 17.5   PHASE
PM 17.5   PM
FM 6.18   FM

0   0.65   1.3   1.95   2.6   3.25   3.9   4.55   MILLISECONDS

ROUND TRIP TRAVEL TIME FROM TRANSMITTER AT C-LEFT

0   10   20   30   40   50   60   70   FT.

ROUND TRIP DISTANCE (BASED ON AVG. VELOCITY OF 15,300'/SEC)

(b) Correlation Peaks as a Function of Travel Time

P-41 619 2

Figure 6-16 – Cross-Correlation of Signals Detected at C-Left

CROSS-CORRELATION
OUTPUT WITH
EXCITATION
PULSE FOR THE
400 μSEC PM PULSE
AT 7.75 kHz

CROSS-CORRELATION
OUTPUT WITH
PHASE DETECTION
WAVEFORM FOR THE
400 μSEC PM PULSE
AT 7.75 kHz

| 0 | 0.975 | 1.95 | 2.925 | 3.9 | 4.875 |
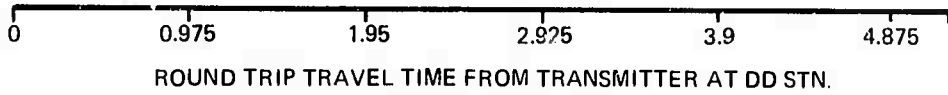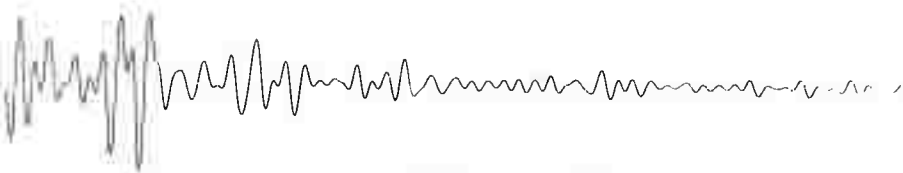
ROUND TRIP TRAVEL TIME FROM TRANSMITTER AT DD STN.

(a) Correlation Results

S-SURFACE WAVE

P-P REF. FROM DESTRESSED ZONE

P-P REF. FROM REFLECTION ZONE IN THE INTERIOR

SHEAR REFLECTION FROM TUNNEL AND DISCONTINUITIES IN DESTRESSED ZONE

P-P REF. FROM AIR-INTERFACE C-LEFT

EXCITATION | CORRELATION FUNCTION

PM 17.5 | PHASE

PM 7.75 | PHASE

PM 17.5 | PM

PM 7.75 | PM

| 0 | 0.65 | 1.3 | 1.95 | 2.6 | 3.25 | 3.9 | 4.55 | 5.15 MILLISEC. |

ROUND TRIP TRAVEL TIME FOR TRANSMITTER AT DD STN

| 0 | 10 | 20 | 30 | 40 | 50 | 60 | 70 FT. |

ROUND TRIP DISTANCE (BASED ON AVG. VELOCITY OF 15,300'/SEC)

(b) Correlation Peaks as a Function of Travel Time

P-41 619-2

Figure 6-17 – Cross-Correlation of Signals Detected at DD Stn

reflecting layer or zone. Tentatively, the cause of this correlation zone has been identified as a reflection zone in the interior of the site.

Comparison of the results shown in Figures 6-16(b) and 6-17(b) shows that correlations from the reflection zone in the interior can be made consistent if the reflection zone is assumed to be located as shown in Figure 6-6. This reflection zone is probably the fracture zone that is in the middle of the tunnel between C-left and DD Stn. This reasoning is supported by the fact that this fracture zone seen from the outside had not been observed to emerge at any other point in the tunnel.

These correlated data show that the presence of destressed zones, the reflection zone in the interior, and also the air-rock interface (which is about 30 feet from the transmitting face) can be detected from either side of the test site, despite the fact that the test site has destressed zones and is full of jointed rocks.

In a practical application, correlation data [such as those presented in Figures 6-16(a) and 6-17(a)] can be stacked to enable the peaks of interest to be discerned. When several correlation results (obtained at consecutive fixed intervals of time and distance) are stacked, the correlation peaks due to discontinuities ahead of the excavation face should appear to be moving with the average speed of the machine. On the other hand, the stacked correlation peaks due to undesired signals (such as direct surface waves and reflected surface waves) should appear to stand still. This stacking method, therefore, would increase the confidence level of data interpretation by allowing the undesired signals to be rejected.

SECTION 7

CONCLUSIONS AND RECOMMENDATIONS

7.1 CONCLUSIONS

The feasibility study program (phase I) has been successfully completed. This investigation has shown that a reflecting interface (a fault or fracture zone) in homogeneous hard rock can be detected. Also, with a reasonable level of confidence, discontinuity interfaces as far away as 30 feet at a field test site compatible to the objectives of the program could be identified using cross-correlation techniques for signal processing.

In summary, the results of this study go an appreciable way toward proving the feasibility of using acoustic techniques for detecting large geologic anomalies ahead of an excavation face. Further development work is needed to optimize an operating system in a hard rock environment where excavation machines are used for tunneling.

7.2 RECOMMENDATIONS

7.2.1 System Requirements

The rate-of-advance of the next generation excavation equipment has been projected to be about 200 feet per day. It will be very desirable to have a detection system that could predict the presence of geological anomalies within this range. Unfortunately, a detection system capable of predicting anomalies in hard rock that far away with a reasonable level of confidence is beyond the existing technology. However, with existing acoustic technology, geological anomalies within a working range of a few tens-of-feet in hard rock can be predicted in real time with a reasonable level of confidence. Bendix Research Laboratories feel that an acoustic system based on this range is adequate for the proposed application, provided that the range data are periodically updated by probing the excavation face every few feet.

At present, we do not know what the next generation machines will look like, but if they are similar to those used today, the transmitting and receiving transducers could be retractably mounted on the cutting head of the machine. The periodic sampling of the excavation face at every few feet would be carried out at each tunneling machine stop, when the body of the machine is being advanced for the next tunneling operation while the cutting head is stationary. In a sense, the data from successive measurements would be stacked to improve detection.

Because of continuous updating of anomaly range data within the prediction range, the confidence level in the proposed detection procedure is expected to be greater than the one where anomalies are detected over a range of a few hundred feet by a single probing of the excavation face.

7.2.2 Recommended Detection System

The recommended detection system is based on acoustic pulse-reflection methods. The underlying principle is to: transmit a frequency-modulated (FM) acoustic signal into rock by exciting the transmitting transducer with an electrical FM pulse, detect the return signal, and process the return signal by a cross-correlation function which closely resembles the expected reflected signal. The cross-correlation method of signal processing can be used to pick out reflected signals that are otherwise unidentifiable in the detected signal. It is proposed that an FM excitation pulse, modified to compensate for the system characteristics, be used for cross-correlation since the signal reflected from a discontinuity will be related to the excitation FM waveform, although it will be highly modified by the characteristics of the transmitter, the receiver, and the rock medium. The reason for choosing an FM acoustic pulse over other possible signals is that the cross-correlated output is much sharper for FM than for any other signals having the same pulse width. The desirable design characteristics of such a system are:

- FM pulse excitation of the sound source at frequencies from
  - 5 to 15 kHz for deep discontinuities (for example, 15-50 feet) which would give a resolution of about 3 feet.

- 15 to 45 kHz for shallow discontinuities (for example, 5-15 feet) which would give a resolution of about 1 foot.

- The use of a simple array of receivers.
- The use of thickness-mode, piezoelectric ceramic transducers, having resonant frequencies well above the highest operating frequency.
- The use of a contained fluid to couple acoustic signals from the transducer to the rock face.
- The use of cross-correlation methods of signal processing with the modified transmitter excitation pulse.

7.2.3 Recommendations for Phase II

Based on the results of phase I, a prototype ultrasonic geologic detection system should be designed and fabricated. The design has to be suitable for use in conjunction with actual material excavation. The assembled prototype system should be experimentally evaluated at two different excavation sites. The system design should have the necessary flexibility for optimizing the signal processing. Although no field test is proposed for a prototype system mounted on an excavation machine, the aim of this program should be to design a system compatible with excavation machines and their surroundings.

SECTION 8

REFERENCES

1. J. E. White, <u>Seismic Waves: Radiation, Transmission and Attenuation</u>, McGraw Hill, New York, 1965, Chap. 3.

2. S. P. Clark, Jr., Ed., <u>Handbook of Physical Constants</u>, Geological Society of America, Inc., New York, 1966, Sections 1, 8 and 9.

3. R. R. Gupta, "Seismic Determination of Geological Discontinuities Ahead of Rapid Excavation," Semiannual Technical Report, Report No. 6051, Nov. 1971, Bendix Research Laboratories, Southfield, Michigan.

4. J. R. Fredrick, <u>Ultrasonic Engineering</u>, John Wiley, New York, 1965, pp. 66-67.

5. L. E. Kinsler and A. R. Frey, <u>Fundamentals of Acoustics</u>, John Wiley and Sons, New York, 1962. Section 6.5.

6. R. C. McMaster, <u>Nondestructive Testing Handbook</u>, Ronald Press, New York, 1959, Vol. II.

7. Research Laboratories Proposal No. 5525, "Seismic Determination of Geological Discontinuities Ahead of Rapid Excavation," submitted to U.S. Bureau of Mines, Twin Cities, Minnesota, August 1970.

8. V. C. Anderson, "Digital Array Phasing," <u>Journal of the Acoustical Society of America</u>, 32, 7, 867 (July 1960).

9. P. Rudnick, "Small Signal Detection in DIMUS Array," <u>Journal of the Acoustical Society of America</u>, 32, 7, 871 (July 1960).

10. V. C. Anderson, "DICANNE, A Reliable Adaptive Process," <u>Journal of the Acoustical Society of America</u>, 45, 2, 398 (1969).

11. Clevite Corporation, "The Design of Piezoelectric Sandwich Transducers," Technical Paper TP-235.

12. C. F. Johnson, "Delineation of Mine Roof Defects by an Ultrasonic Technique," presented at the Conference on the Underground Mining Environment, October 22-29, 1971, University of Missouri, Rolla, Missouri.

13. Y. W. Lee, <u>Statistical Theory of Communication</u>, John Wiley & Sons, Inc., New York, 1960, pp. 289-322.

14. P. N. Keating, Private Communication, 1972.

APPENDIX A
RANGE-FREQUENCY RELATIONSHIP

RANGE EQUATION

With the assumptions made in Section 4.4, the peak (steady-state) acoustic power p_t(watts) radiated by the half-wave resonance sandwich transmitter is given by*

$$p_t = 4 \left(\bar{\alpha}_t^2 \right) \left(V_t^2 \right) \left(\eta_t^{ea} \right) \left(\eta_t^c \right) \Big/ z_r \qquad \text{(A-1)}$$

where the subscript t or r on a quantity denotes whether it is related to the transmitting or receiving transducer, and

$\bar{\alpha}$ = transformation factor relating mechanical to electrical quantities (Coulomb/meter) = $\dfrac{A\ e_{33}}{\ell}$

ℓ = thickness of the piezoelectric material (meter)

A = face area of the transducer (meter^2)

e_{33} = piezoelectric stress constant, relating a field strength in the direction 3 to the stress component in the direction 3 (the electric field is assumed to be along direction 3)

V = peak electrical pulse voltage

z_r = radiation impedance of the propagating rock medium
   $\simeq A_t\ \rho_r\ v_r\ [R_1\ (2k_o\ a_t) + X_1\ (2k_o\ a_t)]$

ρ_r = density of the propagation medium (kilograms/meter^3)

v_r = sound velocity in the rock medium (meter/sec)

k_o = $2\pi/\lambda$

λ = signal wavelength (meter)

---

*T. F. Heuter and R. H. Bolt, <u>Sonics</u>, John Wiley, New York, 1955, Chapter 4.

a_t = transducer radius

R_1 and X_1 are mathematical functions which can be found in any textbook

η^{ea} = electro-acoustic transducer efficiency

η^c = coupling efficiency of the acoustic couplant

The intensity I_t of the radiated signal at a radial distance L then becomes

$$I_t = \frac{P_t^2}{2 \, \rho_r \, v_r} = \frac{P_t}{4\pi L^2} \, D_t \qquad (A-2)$$

where

p = peak pressure (newton/meter^2)

D = directivity of a transducer = $\dfrac{4\pi A}{\lambda^2}$

At the operating frequencies of interest, the signal amplitude of sound waves is predominantly attenuated by frictional losses which is expressed by

$$\exp(-\alpha L) \qquad (A-3)$$

where $\alpha (=a_p f)$ is the attenuation coefficient (meter^{-1}) of the rock medium and f is the signal frequency.

The expression for the peak pressure p_r at the receiving transducer (located in close proximity to the transmitter) becomes

$$p_r = \frac{2\bar{a}_t \, v_t \left(\sqrt{\eta_t^{ea} \, \eta_t^c \, \eta_r^c} \right) R(\theta) \, \exp(-2a_p fL)}{\sqrt{R_1 (2ka)} \, 2L\lambda} \qquad (A-4)$$

where $R(\theta)$ is the reflection coefficient at the reflecting interface as a function of incident angle θ.

The open-circuit peak voltage v_r across a nonresonant receiver will then be

$$V_r = \frac{\bar{\alpha}_t \, A_r}{\bar{\alpha}_r} \left(\frac{k_c^2}{1 + k_c^2} \right) R(\theta) \left(\frac{\sqrt{\eta_t^{ea} \, \eta_c^e \, \eta_r^c \, \eta_r^{ae}}}{L\lambda \, \exp(2a_p fL)} \right) \quad \text{(A-5)}$$

where η_r^{ae} is the acoustic-to-electric coupling efficiency of the receiver and k_c^2 is the electromechanical coupling coefficient of the piezoelectric receiver material.

For a pulse-modulated continuous wave (PM-CW) pulse-reflection detection system, the steady-state, open-circuit peak voltage across a nonresonant receiver can be simplified to

$$V_r = C_1 \left[\frac{A_t \, V_t \, R(\theta) \, f}{L_d \, v_r \, \exp(2a_p fL)} \right] \quad \text{(A-6)}$$

where C_1 is the constant of the system which is a function of rock and coupling media characteristics and transmitting and receiving transducers, and L_d is the depth of the discontinuity interface below the excavation face.

RECEIVER NOISE

The noise detected in the received signal would be due to contributions from lattice vibrations in the acoustic detector and from conventional noise of the receiving preamplifier.

The acoustic noise intensity I^ℓ due to lattice vibrations is given by[**]

$$I^\ell = 430 \ kT \ \Delta f \ \frac{f^2}{v_m^2} \qquad (A-7)$$

where

k = Boltzman constant

T = temperature (in Kelvin)

Δf = bandwidth of the acoustic signal

v_m = particle sound velocity in the receiver material

The peak electrical noise voltage $V_r{}^\ell$ due to the lattice vibrations can be reduced to

$$V_r{}^\ell = C_2 \frac{f}{\sqrt{L_{min}}} \qquad (A-8)$$

where L_{min} is the depth of the closest discontinuity that can be detected by a PM-CW pulse of bandwidth Δf, and C_2 is a constant which is a function of receiver and rock properties. For a PZT-4 nonresonant receiver (1/8-inches thick), the noise voltage due to lattice vibrations can be approximated by

$$V_r \approx \frac{1.2 \times 10^{-8} \ f \ (kHz)}{L_{min} \ (meter)^{1/2}} \quad \text{Volts} \qquad (A-9)$$

[**] A. Korpel and L. W. Kessler, "Comparison of Methods of Acoustic Holography," Acoustical Holography, Vol. 3 (ed. A. F. Metherell), Plenum Press, New York, 1971. (The referenced equation is an order of magnitude larger than Korpel's result since Korpel's derivation does not include the effects of shear vibrations that are present in solid materials).

This noise voltage would be about 1/2 of a microvolt at f = 30 kHz for a system designed to detect discontinuities at no closer than 1 meter from the excavation surface.

At operating frequencies of interest, the noise voltage contributed by a preamplifier is expected to be relatively insignificant and therefore it will be neglected in further calculations.

Figure 4-1 shows the maximum distance up to which a discontinuity can be detected as a function of frequency in a granite rock by a PM-CW reflection system. In these results, it was assumed that (1) the system bandwidth is 3 kHz which corresponds to a transmitted signal pulse duration of about 300 microseconds, (2) the transmitter is a half-wavelength-thick sandwich (which has 1/8-inch thick PZT-4 discs), (3) both transmitter and receiver face diameters are 2 inches, and (4) the minimum reflected signal voltage is at least ten times as large as the noise voltage. These curves are drawn as a function of a signal frequency f for two extreme values of the attenuation coefficients: namely, low-loss (α = 3.9 x 10^{-6} f sec/m, or Q = 125) and high-loss (α = 27 x 10^{-6} f sec/m, or Q = 20).

APPENDIX B

CROSS-CORRELATION WITH PHASE DETECTION WAVEFORM

In this appendix, we will examine the effect of cross-correlating a phase-shifting wave function $f_1(t)$ with a phase-detection waveform $f_2(t)$. Let $f_1(t)$ have a phase change of ϕ radians at time t equal to zero:

$$f_1(t) = \cos \omega t \, [1 - u(t)] + \cos (\omega t + \phi) \, u(t) \qquad (B-1)$$

where

$$u(t) = 1 \text{ for } t > 0$$
$$\qquad = 0 \text{ for } t < 0$$

For the cross-correlating phase-detection waveform $f_2(t)$, we would like to choose a pulse waveform that is sensitive to changes in phase of $f_1(t)$. Such a pulse waveform $f_2(t)$ should have a phase change of about 180 degrees in the middle of the function. A possible choice for $f_2(t)$ is given by

$$f_2(t) = e^{-\alpha^2 t^2} \cos \omega t \sin \beta t \qquad (B-2)$$

The function $\sin \beta t$ provides the desired phase change at $t = 0$. A Gaussian envelope function has been assumed. The parameters α and β (to be chosen), respectively, govern the effective pulse width of $f_2(t)$ and the change of phase in the middle of $f_2(t)$.

The cross-correlation $C_{12}(\tau)$ is given by

$$C_{12}(\tau) = \frac{1}{2T} \lim_{T \to 0} \int_{-T}^{T} dt\, f_1(t)\, f_2(t + \tau)$$

$$= \int_{-\infty}^{\infty} dt\, e^{-\alpha^2 t^2} \cos \omega t \, \sin \beta t \, \{\cos \omega\, (t + \tau)\, [1 - u\, (t + \tau)] + \cos\, [\omega\, (t + \tau) + \phi]\, u\, (t + \tau)\}$$

$$= \frac{1}{2} \int_{-\infty}^{\infty} dt\, e^{-\alpha^2 t^2} \, [\sin\, (\beta + \omega)\, t + \sin\, (\beta - \omega)\, t] \, \{\cos \omega\, (t + \tau)\, \{1 - u\, (t + \tau)\} + \cos\, [\omega\, (t + \tau) + \phi]\, u\, (t + \tau)\}$$

$$= \frac{1}{2} \int_{-\infty}^{-\tau} dt\, e^{-\alpha^2 t^2} \, [\sin\, (\beta + \omega)\, t + \sin\, (\beta - \omega)\, t] \, \cos \omega\, (t + \tau)$$

$$+ \frac{1}{2} \int_{-\tau}^{\infty} dt\, e^{-\alpha^2 t^2} \, [\sin\, (\beta + \omega)\, t + \sin\, (\beta - \omega)\, t] \, \cos\, [\omega\, (t + \tau) + \phi]$$

$$= \frac{1}{4} \int_{-\infty}^{-\tau} dt\, e^{-\alpha^2 t^2} \, \{\sin\, [(\beta + 2\omega)\, t + \omega\tau] + \sin\, (\beta t - \omega\tau) + \sin\, (\beta t + \omega\tau) + \sin\, [(\beta - 2\omega)\, t - \omega\tau]\}$$

$$+ \frac{1}{4} \int_{-\tau}^{\infty} dt\, e^{-\alpha^2 t^2} \, \{\sin\, [(\beta + 2\omega)\, t + \omega\tau + \phi] + \sin\, (\beta t - \omega\tau - \phi) + \sin\, (\beta t + \omega\tau + \phi) + \sin\, [(\beta - 2\omega)\, t - \omega\tau - \phi]\} \qquad \text{(B-3)}$$

In the limit $\tau \to \infty$, the first term in equation (B-3) vanishes and the equation reduces to

$$\frac{1}{4} \sin(\omega\tau + \phi) \int_{-\infty}^{\infty} dt\, e^{-\alpha^2 t^2} \{\cos(\beta + 2\omega)t - \cos(\beta - 2\omega)t\} \quad \text{(B-4)}$$

since the terms in $\cos(\omega\tau + \phi)$ vanish through symmetry in the range of integration. The integral is now just a pair of Fourier transforms, and we obtain

$$\frac{\pi^{1/2}}{4\alpha} \sin(\omega\tau + \phi) \left[e^{-\frac{(2\omega + \beta)^2}{4\alpha^2}} - e^{-\frac{(2\omega - \beta)^2}{4\alpha^2}} \right] \quad \text{(B-5)}$$

Thus,

$$C_{12}(\tau \to \infty) = \frac{-\pi^{1/2}}{2\alpha} \sin(\omega\tau + \phi)\, \sinh\left(\frac{\omega\beta}{\alpha^2}\right) e^{-(\omega^2 + \beta^2/4)/\alpha^2} \quad \text{(B-6)}$$

A similar result for $\tau \to -\infty$ is obtained (but with $\phi = o$).

In the limit $\tau \to o$, equation (B-3) becomes

$$\frac{1}{4}(\cos(\omega\tau + \phi) - 1) \int_{o}^{\infty} dt\, e^{-\alpha^2 t^2} \{\sin(2\omega + \beta)t$$

$$\text{(B-7)}$$

$$+\ 2\sin\beta t - \sin(2\omega - \beta)t\}$$

$$+\ \frac{1}{4}\sin(\omega\tau + \phi) \int_{o}^{\infty} dt\, e^{-\alpha^2 t^2} \{\cos(2\omega + \beta)t - \cos(2\omega - \beta)t\}$$

The last term gives essentially half of equation (B-4)(with $\tau \to o$, of course). The first term is

$$
-\frac{i\pi^{1/2}}{8\alpha}(\cos\phi - 1)\left\{ e^{-\frac{(2\omega+\beta)^2}{4\alpha^2}}\text{Erf}\left(\frac{i(2\omega+\beta)}{2\alpha}\right)\right.
$$

$$
+2e^{-\frac{\beta^2}{4\alpha^2}}\text{Erf}\left(\frac{i\beta}{2\alpha}\right) \tag{B-8}
$$

$$
\left. -e^{-\frac{(2\omega-\beta)^2}{4\alpha^2}}\text{Erf}\left(\frac{i(2\omega-\beta)}{2\alpha}\right)\right\}
$$

Since $\omega^2 \gg \alpha^2$ or β^2, the largest term in equation (B-8), and also equation (B-7), is

$$
-\frac{i\pi^{1/2}}{8\alpha}(\cos\phi - 1)\cdot 2e^{-\frac{\beta^2}{4\alpha^2}}\text{Erf}\left(\frac{i\beta}{2\alpha}\right) \tag{B-9}
$$

which, if $\alpha > 3\beta$, approximates to

$$
\sim \frac{\beta}{4\alpha^2}(\cos\phi - 1)e^{-\frac{\beta^2}{4\alpha^2}} \tag{B-10}
$$

Thus,

$$
C_{12}(\tau \sim o) \sim \frac{-\beta}{4\alpha^2}(1 - \cos\phi)e^{-\frac{\beta^2}{4\alpha^2}} \tag{B-11}
$$

Hence, the value of the amplitude of $C_{12}(\tau)$ around $\tau = o$ is larger than its value at large values of $|\tau|$ by a factor in the order of

$$\frac{\beta}{\alpha\pi^{1/2}} e^{\frac{\omega^2}{4\alpha^2}} \cosh\left(\frac{\omega\beta}{\alpha^2}\right) , \qquad (\text{B-12})$$

which is large when $\omega^2 \gg \alpha^2$.

This result shows that the cross-correlation function is small except near $\tau = o$ where the phase shift occurs in the function $f_1(t)$. Hence, this type of cross-correlation can find phase changes in a function.

An example of the effectiveness of cross-correlating a simple sinusoidal function $f_1(t)$ with a phase-detection waveform $f_2(t)$ is shown in Figure 6-14.